

Neurovascular Coupling Equations for Code version 3.1 with  
**Wilson and Cowan Population Neuron**

Tim David

July 24, 2019

## **Todo list**

|  |    |
|--|----|
| The above equation for $K_i^+$ is redundant since it is not used anywhere else in the SMC. We can use it but it would make any difference. . . . . | 33 |
| do we use calcium ( $\text{Ca}^{2+}$ )-calmodulin complex at all? . . . . .  | 40 |

## **Contents**

|   |           |
|---|-----------|
| <b>1 Results from Wilson and Cowan model</b>          | <b>9</b>  |
| <b>2 Interneuron Modeling</b>                         | <b>15</b> |
| <b>3 Equations and Parameters</b>                     | <b>19</b> |
| <b>4 Blood-oxygen-level dependent (BOLD) response</b> | <b>24</b> |
| <b>5 Synaptic Cleft and Astrocyte</b>                 | <b>26</b> |
| <b>6 Perivascular space (PVS)</b>                     | <b>31</b> |
| <b>7 Smooth muscle cell (SMC)</b>                     | <b>32</b> |
| <b>8 Endothelial cell (EC)</b>                        | <b>37</b> |
| <b>9 Nitric oxide (NO) pathway</b>                    | <b>39</b> |
| <b>10 AA 20-HETE NO pathway</b>                       | <b>43</b> |
| <b>11 Wall mechanics</b>                              | <b>45</b> |
| <b>12 Tissue Slice Model</b>                          | <b>46</b> |
| <b>13 Initial values</b>                              | <b>47</b> |
| Bibliography  | 48        |

## Introduction

The single neurovascular unit (NVU) model originally developed by Farr and David [4] and later extended by Dormanns et al. [3], Dormanns et al. [2], Mathias et al. [13], Kenny et al. [8], Mathias et al. [12] and most recently by Kenny (unpublished) contains 51 ordinary differential equations (ODEs) plus a large number of algebraic variables and parameters. The equations and parameters are divided into sections corresponding to different compartments and pathways of the model. Figure 1 shows the current status of the new more simplified neuron/full model (see below for details).

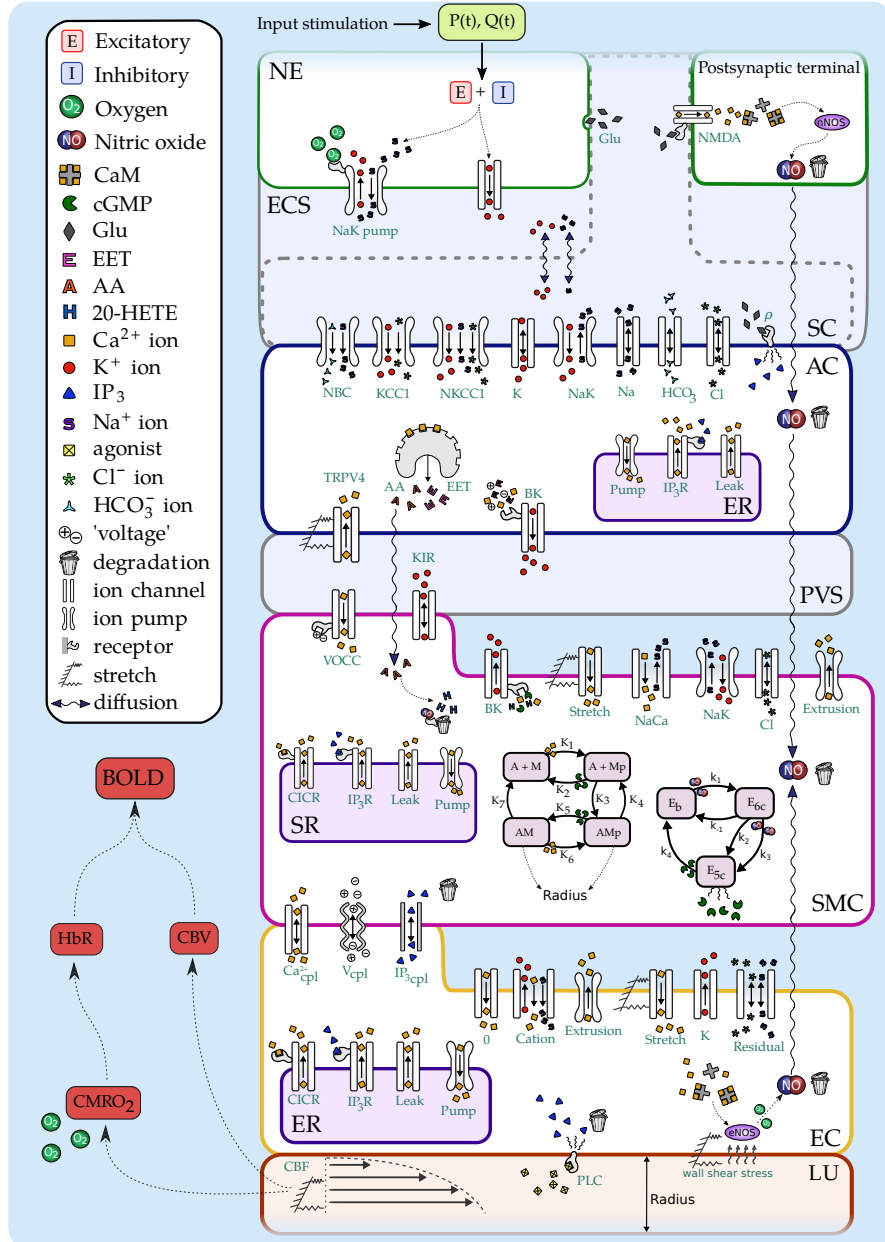


Figure 1: **FULL** NVU 3.1 including BOLD pathway and Wilson and Cowan neuron model

The difficulty in analysing the single neuron model to produce a viable simulation of the Berwick mouse experimental data (HbT/O/R) has encouraged us to look at both neural mass models (which essentially produce oscillations modelling

$\alpha$  and  $\beta$  waves = EEG data) and the work of Wilson and Cowan (especially their seminal 1972 paper see Biophys Jour 12 (1-24), 1972) . We concentrate here on the Wilson Cowan model (designated CW hereafter) for the time being. The derivation of the model is reproduced here for clarity and to ensure a thorough understanding of the model and its appropriateness. We define the following

- $E(t)$  = proportion of excitatory cells firing per unit time at time  $t$
- $I(t)$  = proportion of inhibitory cells firing per unit time at time  $t$

$E(t)=I(t)=0$  is considered the resting state and note that both  $E(t)$  and  $I(t)$  can become negative at some time.

Suppose refractory period of excitable cells is  $r$  msec, then the proportion of cells that are in a refractory state is given by

$$\int_{t-r}^r E(\tau) d\tau \quad (1)$$

thus cells which are sensitive are defined as

$$1 - \int_{t-r}^r E(\tau) d\tau \quad (2)$$

Similarly for  $I(t)$ . We define the expected proportions of either  $E(t)$  or  $I(t)$  (subpopulations) receiving at least threshold excitation per unit time as a function of the average levels of excitation within the subpopulations by  $\mathfrak{S}_e(x)$  and  $\mathfrak{S}_i(x)$ . Suppose a distribution function  $\mathfrak{D}$  of individual thresholds for the subpopulation then

$$\mathfrak{S}(x) = \int_0^{x(t)} \mathfrak{D}(\theta) d\theta \quad (3)$$

where  $x(t)$  is the average excitation OR

$$\mathfrak{S}(x) = \int_{\frac{\theta}{x(t)}}^{\infty} \mathfrak{C}(\omega) d\omega \quad (4)$$

where  $\mathfrak{C}(\omega)$  is a distributions of synapses per cell. Both definitions produce (if  $\mathfrak{D}$ ,  $\mathfrak{C}$  are monotonic) an  $\mathfrak{S}(x)$  which is sigmoidal in shape. We can write this as

$$\mathfrak{S}(x) = \frac{1}{1 + \exp[-\gamma(x - \delta)]} \quad (5)$$

Assuming individual cells sum their inputs and the delay from stimulation is  $\alpha(t)$  then the average level of excitation generated will be

$$\int_{-\infty}^t \alpha(t - \tau) [c_1 E(\tau) - c_2 I(\tau) + P(\tau)] d\tau \quad (6)$$

$c_1$  and  $c_2$  represent the average number of excitatory/inhibitory synapses per cell and  $P(\tau)$  is the external input to the excitatory subpopulation. By assuming a "coarse grain" variable defined by

$$\bar{f}(t) = \frac{1}{s} \int_{t-s}^t f(\tau) d\tau \quad (7)$$

and assuming that at time  $t+\tau$  the dynamics of the localised populations are given by

$$E(t + \tau) = \left[ 1 - \int_{t-r}^t E(t') dt' \right] \mathfrak{S}_e(x_e(t)) \quad (8)$$

with  $x(t)$  defined previously, and

$$I(t + \tau) = \left[ 1 - \int_{t-r}^t I(t') dt' \right] \mathfrak{S}_i(x_e(t)) \quad (9)$$

Using Taylor series expansion about  $\tau=0$  gives

$$\begin{aligned}\tau \frac{dE}{dt} &= -\bar{E} + (1 - r\bar{E})\mathfrak{S}_e [kc_1\bar{E} - c_2\bar{I} + kP(t)] \\ \tau' \frac{dI}{dt} &= -\bar{I} + (1 - r\bar{I})\mathfrak{S}_i [k'c_3\bar{E} - c_4\bar{I} + k'Q(t)]\end{aligned}\quad (10)$$

$Q(t)$  is the stimulation of the inhibitory cells and

$$\begin{aligned}\int_{t-r}^t E(t')dt' &= r\bar{E} \\ \int_{-\infty}^t \alpha(t-t')E(t')dt' &= k\bar{E}\end{aligned}\quad (11)$$

With some redefinitions we have the final odes

$$\begin{aligned}\tau_e \frac{dE}{dt} &= -E + (k_e - r_e E)\mathfrak{S}_e [c_1 E - c_2 I + P(t)] \\ \tau_i \frac{dI}{dt} &= -\bar{I} + (k_i - r_i I)\mathfrak{S}_i [c_3 E - c_4 I + Q(t)]\end{aligned}\quad (12)$$

We should note the following . The state  $E=I=0$  should be stable and be a steady state solution to equations for  $P=Q=0$ .  $\mathfrak{S}_e$  and  $\mathfrak{S}_i$  are transformed so that  $\mathfrak{S}_e = \mathfrak{S}_i = 0$ . This gives

$$\mathfrak{S}(x) = \frac{1}{1 + \exp[-\alpha(x - \delta)]} - \frac{1}{1 + \exp(\alpha\delta)} \quad (13)$$

But the maximum values of  $\mathfrak{S}_{e,i}$  will be less than zero and hence  $k_e$  and  $k_i$  are the max values. as defined

$$\lim_{x \rightarrow \infty} \mathfrak{S}(x) = 1 - \frac{1}{1 + \exp(\alpha\delta)} \quad (14)$$

The isoclines for the equations suggest that  $\exists 3$  or possibly  $5$  steady states. With  $P$  and  $Q = 0$  these isoclines have the following form. Here '-' indicates unstable '+' indicates stable. In our case we wish to progress from  $E=I=0$  when  $P=Q=0$  to some stable state with  $P,Q, \neq 0$  and for the system to return to  $E=I=0$ . This is not trivial (see Wilson and Cowan paper). However using the following parameters we have been able to produce a reasonable profile for  $E(t)$  and  $I(t)$

Table 1

| Parameter  | Value   |
|------------|---------|
| $c_1$      | 12      |
| $c_2$      | 10      |
| $c_3$      | 13      |
| $c_4$      | 11      |
| $a_e$      | 1.2     |
| $\theta_e$ | 2.8     |
| $a_i$      | 1.0     |
| $\theta_i$ | 4.0     |
| $r_e$      | 1.0     |
| $r_i$      | 4.0     |
| $\tau_e$   | 10 msec |
| $\tau_i$   | 10 msec |

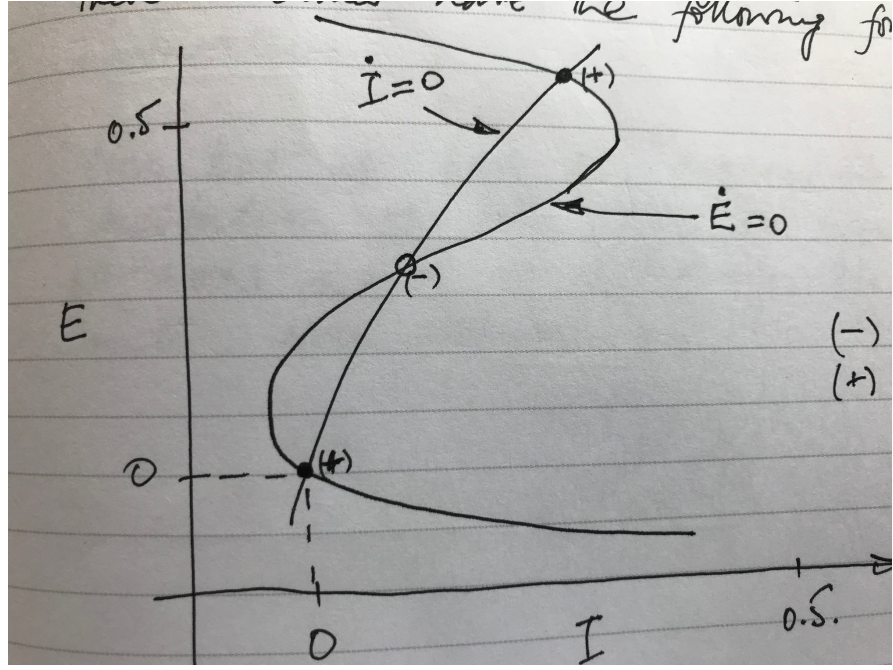


Figure 2: steady states

$k_e = \mathfrak{S}_e(10)$  and  $k_i = \mathfrak{S}_i(10)$  are used to produce maximum values of the sigmoid function. Both  $k_e$  and  $k_i$  are  $\approx 1$ . We should note here that due to the small values of the characteristic time scales  $\tau_e$  and  $\tau_i$  the output for  $E$  and  $I$  are essentially 'square pulses' if the functions  $P$  and  $Q$  are also 'square pulses' and the stimulation period is much larger than  $\tau_e$  or  $\tau_i$ . Figure shows the results of  $E(t)$  and  $I(t)$  for a 2 second stimulation

Note that the horizontal axes are in milliseconds. In order to develop the neuron model further we need to ensure that the more simple model replicates (adequately) the results of the more complex one. It turns out (see below the section in determining the ATP-ase pump) that in order to develop this simple model all that is needed are four outputs, viz.  $K^+$  in the ECS,  $Na^+$  in the soma and dendrite and the time derivative of the  $K^+$  in the ECS.

We show the output of the full model for 2 (Figure 4) and 16 second (Figure 5) stimuli.  $K^+$  in the synaptic cleft is determined from the derivative of the potassium ( $K^+$ ) in the ECS. It is important to make sure that the resulting  $K^+$  replicates adequately the result of Ostby [15], since we know this works !!

It can be seen that the profiles for  $K^+$  and both sodium ( $Na^+$ ) could be modelled using a differential equation of the form

$$\frac{d\phi_i(t)}{dt} + \alpha_i \phi_i(t) = f_i(t) \quad (15)$$

Furthermore  $f_i(t)$  could be found using the profiles of  $E(t)$  and  $I(t)$ . Such that

$$f_i(t) = f_i(E(t) - I(t)) \quad (16)$$

The general solution looks like

$$\phi_i(t) = \frac{f_i(t)}{\alpha_i} (1 - \exp(-\alpha_i t)) \quad (17)$$

or more succinctly

$$\frac{d\phi_i(t)}{dt} + \beta \phi_i = \alpha \beta \quad (18)$$

with solution

$$\phi_i(t) = \alpha (1 - \exp(-\beta t)) \quad (19)$$

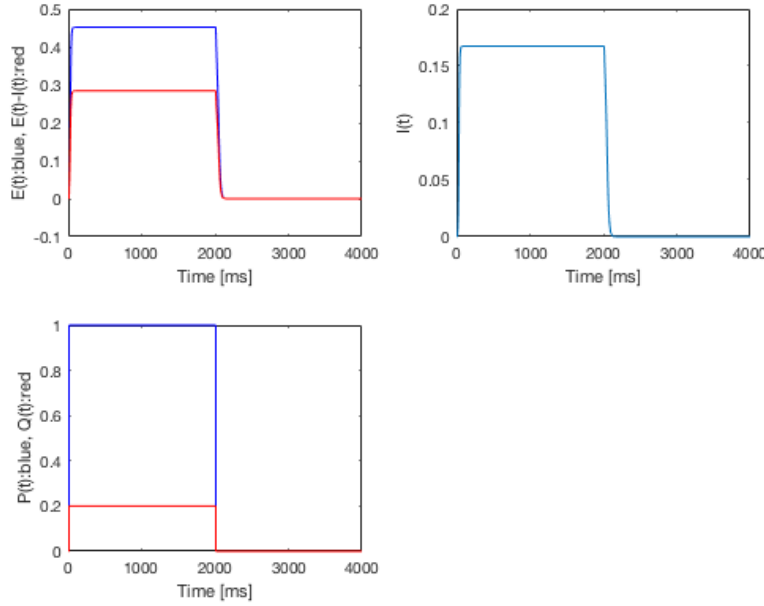


Figure 3: Upper left:  $E(t)$  and  $E(t)-I(t)$ , Upper right:  $I(t)$ . Lower left  $P(t)$  and  $Q(t)$

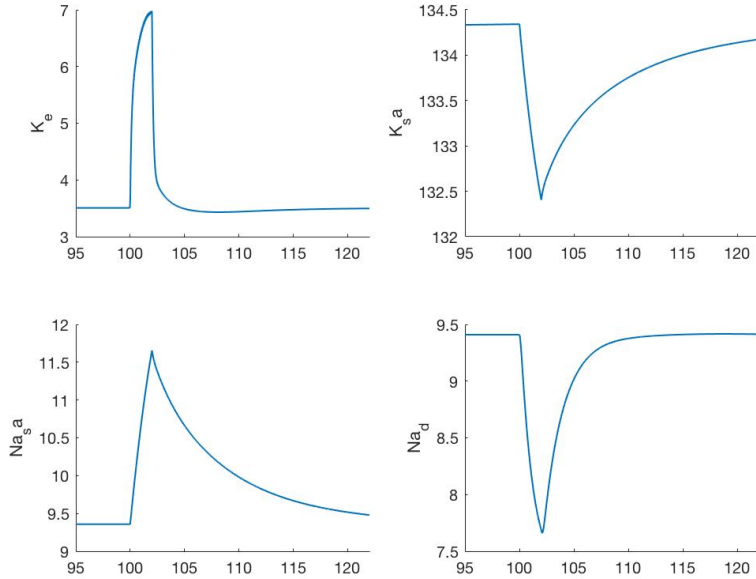


Figure 4: Time-dependent profiles of a 2 sec stimulus for  $K^+$  in the ECS and the synapse of the neuron (top row) and  $Na^+$  in the soma and dendrite (bottom row).

We are now in a position to develop a simple neuron model. Some experiments have provided information with which we can establish adequate values for  $\alpha$  and  $\beta$ . We assume that the forcing function (RHS of ode) is a 'square wave'. We further assume that the stimulus is of the order of  $0.022 \text{ mA cm}^{-2}$ . On this basis the functions modelling  $K^+$  and  $Na^+$

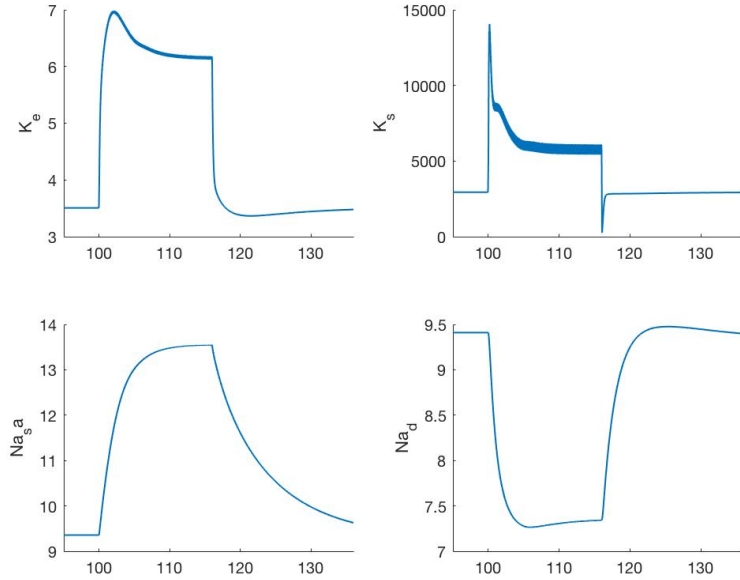


Figure 5: Time-dependent profiles of a 16 sec stimulus for  $K^+$  in the ECS and the synapse of the neuron (top row) and  $Na^+$  in the soma and dendrite (bottom row).

are given by

$$\begin{aligned} [K_e^+] (t) &\simeq 3.5 + 2.7(1 - \exp(-1.5t)) \\ [Na_d^+] (t) &\simeq 9.42 - 2.12(1 - \exp(-0.7t)) \\ [K_{sa}^+] (t) &\simeq 9.37 + 4.23(1 - \exp(-0.65t)) \end{aligned} \quad (20)$$

We now use the values of the parameters listed in Table 1 above and those in equation and find the solution to the time-dependent profiles for  $K_e^+, Na_{sa}^+$  and  $Na_d^+$  using various values of  $P(t)$  to signify a varying stimulus magnitude and the forcing function given by  $\delta(E(t) - I(t))$  where for a stimulus of  $0.022 \text{ mA cm}^{-2}$  the forcing function is of unit magnitude. This value of  $0.022 \text{ mA cm}^{-2}$  was the original value when using the Mathias neuron model. Figures 6 - 8 show the change in concentrations as  $P(t)$  changes magnitude. There is a clear bifurcation at  $P(t) \simeq 0.4$ . This is expected as Wilson and Cowan show that the steady state values traverse from stable through unstable to stable again as  $P(t)$  moves from 0.3 to higher values. As shown in Figure 9. We assume WLOG that  $p(t)=0.5$  corresponds to a stimulus of  $22 \text{ mA cm}^2$ . Varying the value of  $P(t)$  therefore enables the model to vary the stimulus input magnitude.

In the Ostby model the input to the NVU system was essentially a flux of  $K^+$  into the synaptic cleft. In the Mathias neuron model this was achieved by using the derivative of the ECS  $K^+$  multiplied by a constant to take into account the small synaptic volume compared to that of the ECS. We therefore need to determine the time dependent value of  $\frac{dK_e^+}{dt}$ . This is trivial as it is just a rearrangement of the ode given in equation . It is written as

$$\frac{dK_e^+}{dt} = -\beta K_e^+ + \alpha \beta \quad (21)$$

Figure 10 shows the derivative  $\frac{dK_e^+}{dt}$  as a function of time. This should be compared to the Ostby input as shown in Figure 11. Note that the time scales are different but the essential form is similar. And the integrals of the positive value of  $\frac{dK_e^+}{dt}$  is equal to the negative value of  $\frac{dK_e^+}{dt}$  as is the case with Ostby.

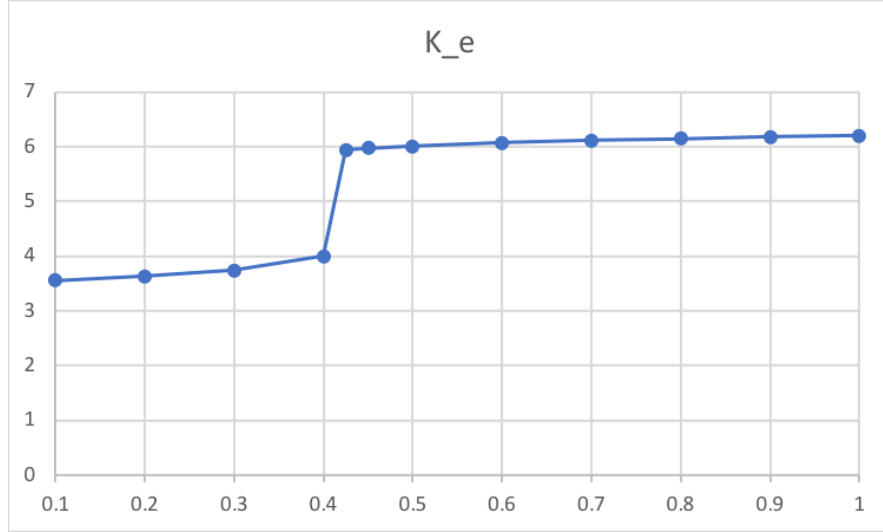


Figure 6:  $K_e$  versus  $P(t)$

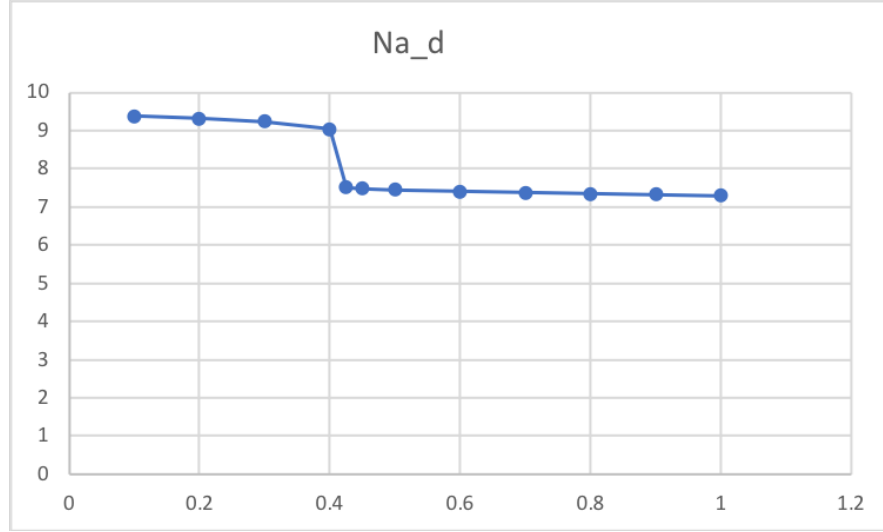


Figure 7:  $Na_d$  versus  $P(t)$

## 1 Results from Wilson and Cowan model

We are now in a position to compare the new neuron model developed from Wilson and Cowan with experimental results from [24]. Firstly Figure 12 shows the excitatory and inhibitory inputs  $E(t)$  and  $I(t)$  resp. All figures show the old model in red and new model in blue. Figure 13 shows the flux of  $K^+$  into the synaptic cleft for the old neuron model [13] (red) compared with the new model (blue). Figure 14 shows the  $K^+$  in the ECS for both models (colours as noted above). Figure 1 shows the  $K^+$  in the synaptic cleft. Figure 16 shows the resulting radius (red: old model, blue: new model) Here we see that the radius now has the correct 'plateau' profile. The rate of increase at the start of the stimulation is the same as the old model. A comparison can be done with the results of [24]. Figure 17 provides the time-dependent profiles of  $\Delta CBF$  for both Zheng and the Wilson/Cowan model. The value of the  $K^+$  in the ECS has been adjusted to make the maximum height of the  $\Delta CBF$  profile fit the experiment. We note a number of issues

- The initial rate of increase of  $\Delta CBF$  is lower than the Zheng result from the experiment

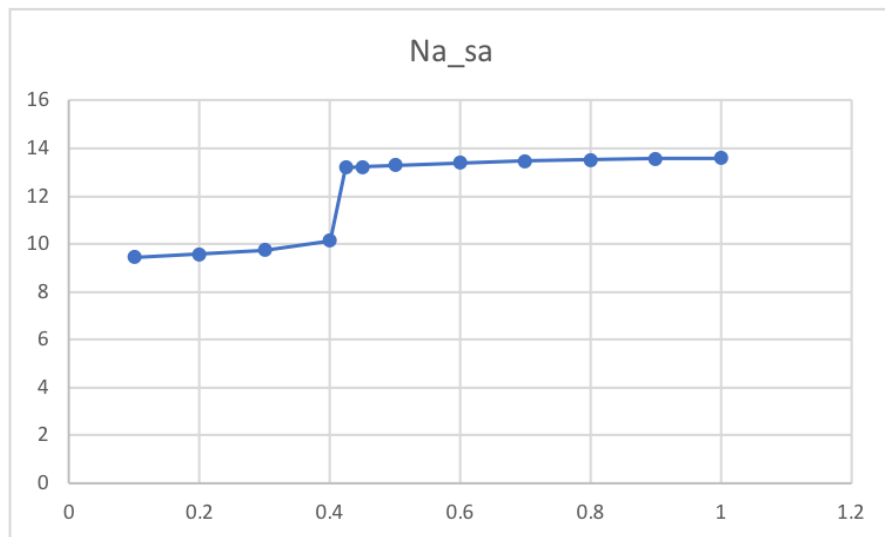


Figure 8:  $Na_{sa}$  versus  $P(t)$

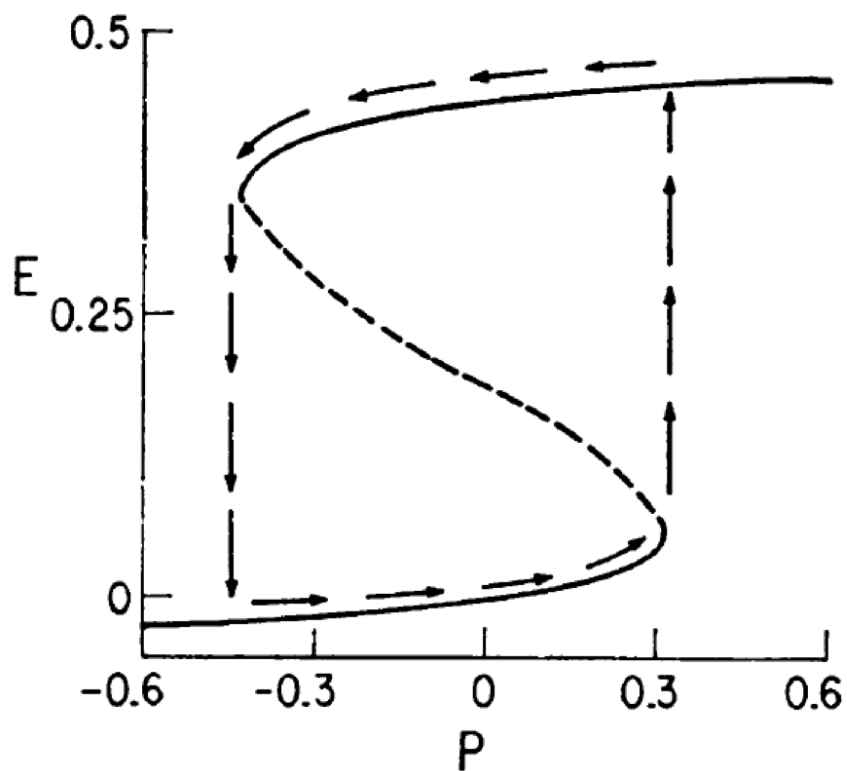


Figure 9: E vs P (taken from Wilson and Cowan paper)

- The decay of the  $\Delta$ CBF is also too long.
- the model profile does not exhibit a 'dip' in the middle of the stimulus.

The  $\Delta$ CBF rates in increase and decay are functions of the radius profile. We are able to change the initial rate and final decay by altering the smooth muscle mechanism. This will be done at a later stage. The 'dip' however can be simulated by investigating the profile of the neuronal input. We show below how this may be achieved.

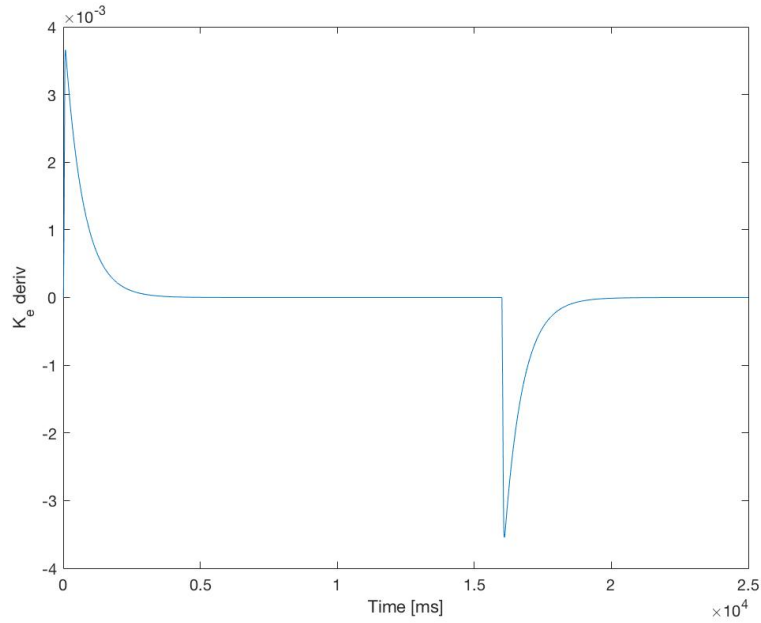


Figure 10:  $\frac{dK_e^+}{dt}$  as a function of time using a stimulation of 16 seconds. re-arrangement of basic  $K^+$  ode, see equation

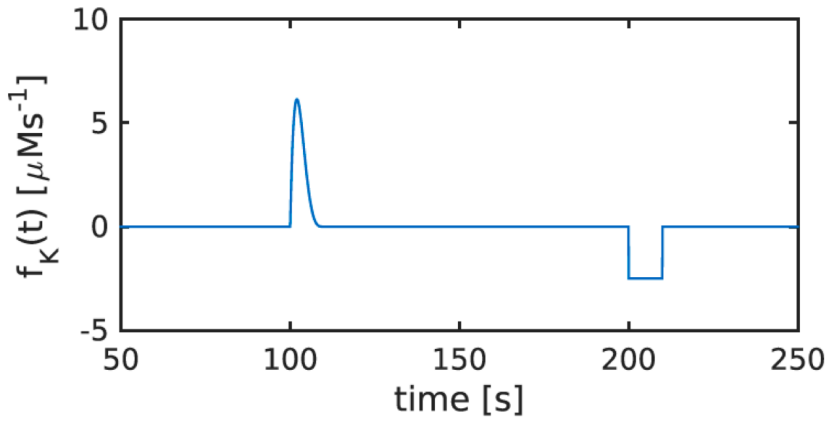


Figure 11: Ostby input (replicating a neuron activation) over 200 seconds, compare with Figure 10

## 1.1 Models of Murine whisker stimulation

Chapter 11 of the book Mathematical Foundations of Neuroscience by Ermentrout and Terman provides a model of the excitatory and inhibitory neurons resulting from thalamic input as a way of describing the stimulation of the somatosensory cortex via the whisker pad. Within the barrel cortex of the rat there exist strong recurrent excitatory and inhibitory networks. These connected networks receive stimulus from the thalamus ( $T(t)$ ). Each neuronal type inhibits the other and themselves.

The experiments seem to show that it is not the peak value of the thalamic input but the time rate of change of the

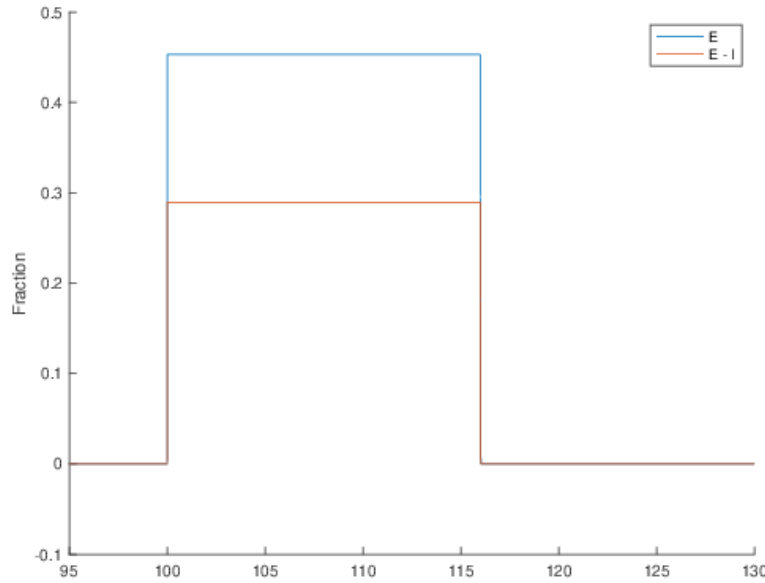


Figure 12:  $E(t)$  and  $I(t)$  for a 16 second stimulation

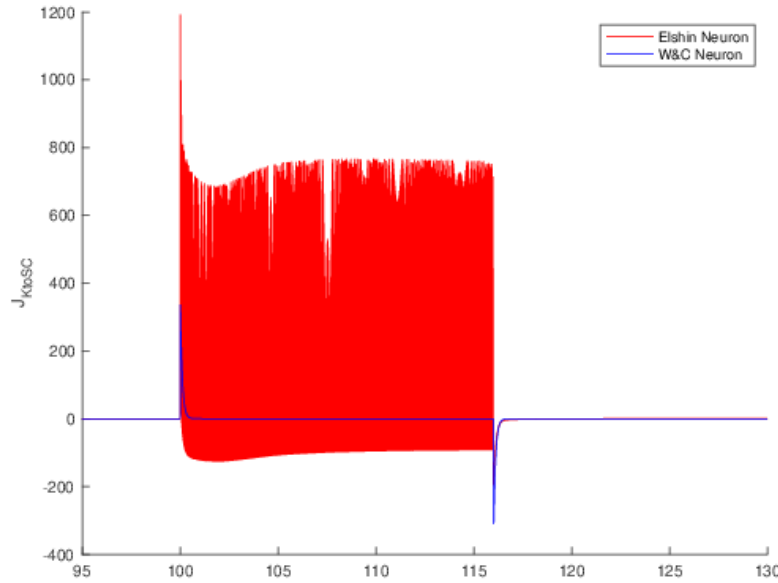


Figure 13: Flux of  $K^+$  into the synaptic cleft (old model red, new model blue)

stimulation. The chapter provides an example whose equations are given below.

$$\tau_e \frac{dE}{dt} = -E + F_e (w_{ee}E - w_{ie} + w_{te}T(t)) \quad (22)$$

$$\tau_i \frac{dI}{dt} = -I + F_i (w_{ei}E - w_{ii} + w_{ti}T(t)) \quad (23)$$

Table 1 (parameters for barrel cortex model)

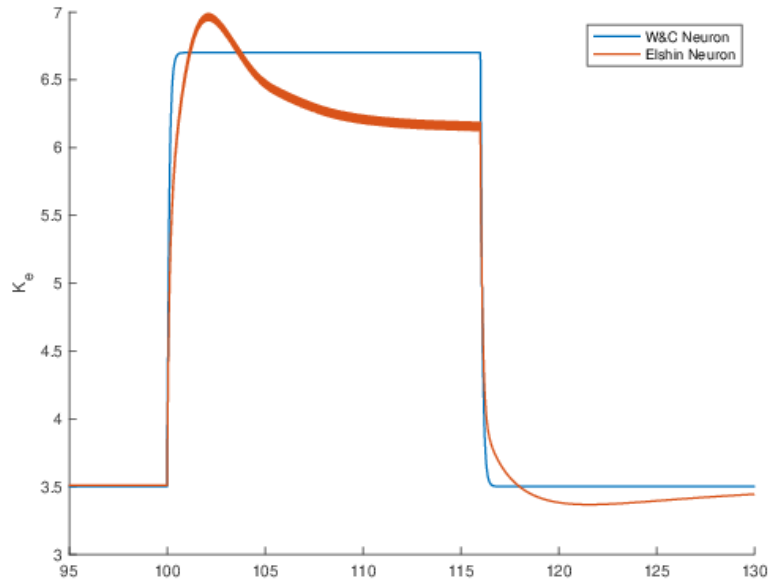


Figure 14:  $K^+$  in the ECS (red: old model. Blue: new model)

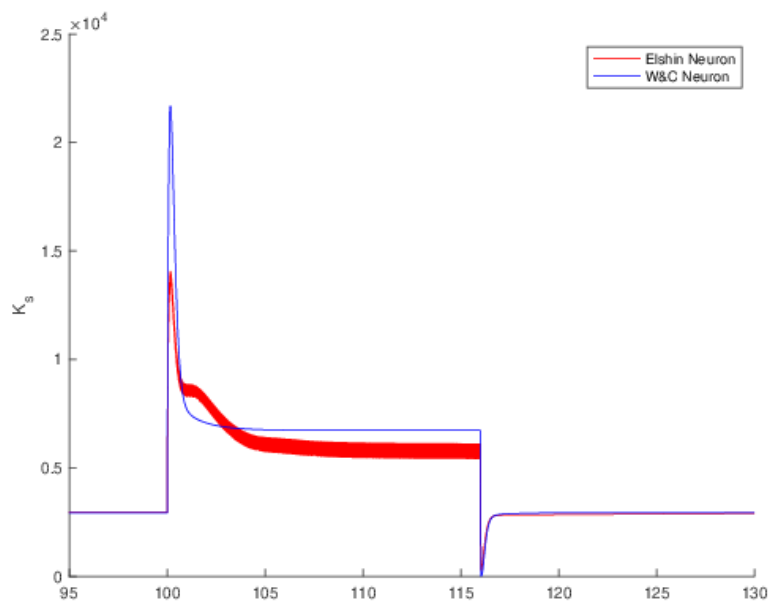


Figure 15:  $K^+(t)$  in the synaptic cleft (red: old model, blue: new model)

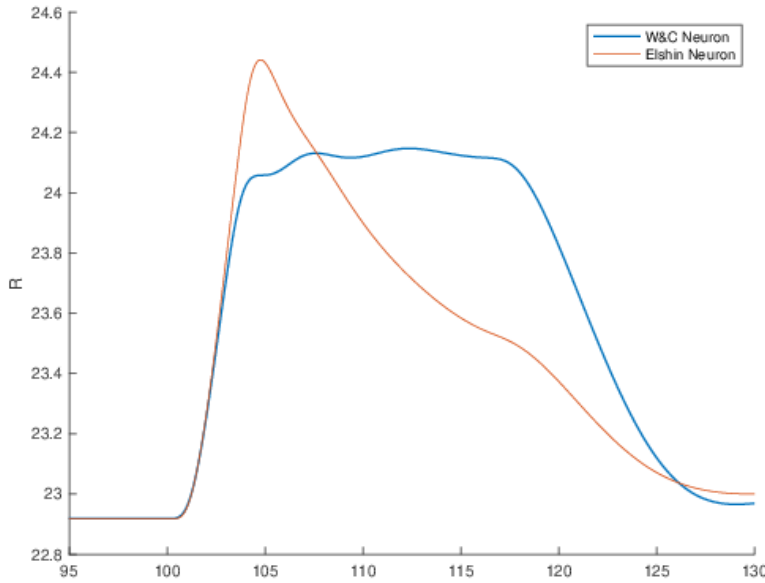


Figure 16: Radius  $R(t)$  for a 16 second stimulus (red: old model, blue: new model)

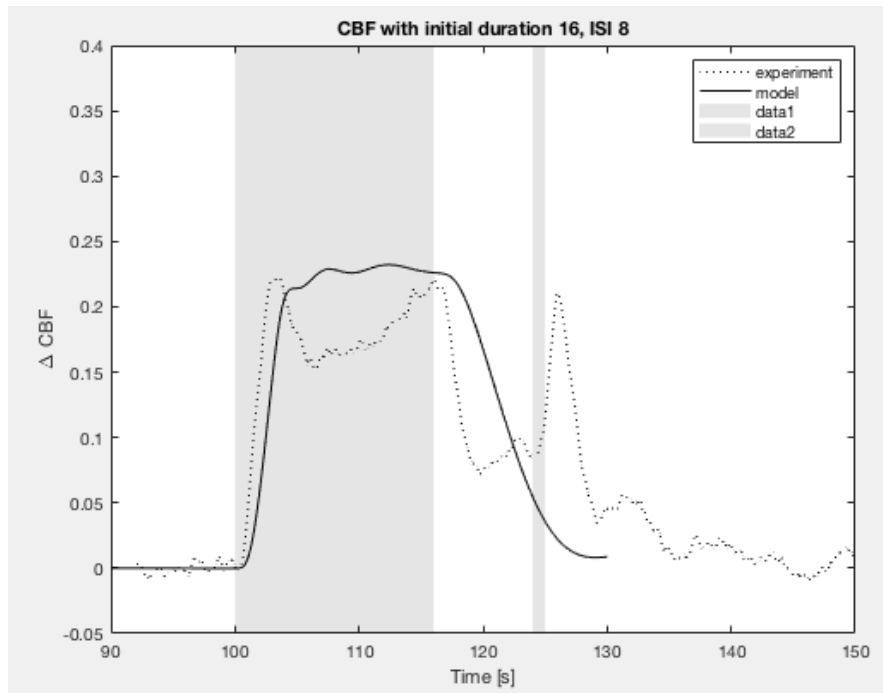


Figure 17: Comparison of old neuron model with new model for  $\Delta\text{CBF}$

|          |       |
|----------|-------|
| $w_{ee}$ | 42    |
| $w_{ie}$ | 24    |
| $e_i$    | 42    |
| $w_{ii}$ | 18    |
| $\tau_e$ | 5     |
| $\tau_i$ | 15    |
| $w_{te}$ | 53.43 |
| $w_{ti}$ | 68.4  |

Along with the gain functions written as

$$F_e(x) = \frac{5.12}{(e^{-x} - e^{-(x+15)} )^2} \quad (24)$$

We should note finally that Ermentrout and Terman show that the factor  $(1 - r_e E)$  makes little difference to the output so it is assumed that both  $r_e$  and  $r_i = 0$ .

To round out the model a thalamic input is needed. Since the rate of increase of input is the signifying factor in whether the firing rate increases a function is needed which simulates a relatively constant max value but a variation in the time taken to reach that value.

## 2 Interneuron Modeling

As part of a collaboration with the Berwick group in Sheffield UK it was decided to create a model of an inhibitory interneuron with  $\gamma$ -aminobutyric acid (GABA) and neuropeptide Y (NPY) to induce dilation when the neuronal vascular response is mediated by GABA but provides constriction with NPY. This is clearly a balance of two competing pathways. To produce a viable model it was agreed that the model should be compared with experimental data from Berwick et al.

An interneuron is a specialised type of neuron whose primary role is to form a connection between other types of neurons. A large majority of interneurons of the central nervous system are of the inhibitory type. In contrast to excitatory neurons, inhibitory cortical interneurons characteristically release the neuro-transmitter GABA [7].

GABA is the main inhibitory neurotransmitter in the mammalian cortex [16]. Every third chemical synapse in the brain uses neurotransmitter GABA as an integral part of the neurotransmission process [17]. In  $GABA_A$  receptors, binding of GABA molecules in the extracellular part of the receptor triggers the opening of a chlorine ( $Cl^-$ ) ion selective pore, where the channel has a reversal potential of about  $-75$  mV in neurons. These receptors are also found on astrocytes [17] and smooth muscle [14].

Losi et al. [11] found that  $GABA_A$  receptors on astrocytes are similar in many, though not all, aspects to those expressed by neurons. One difference is that activation of astrocytic  $GABA_A$  receptors leads to a depolarising current in mature astrocytes, as opposed to mature neurons, due to the  $Na^+/K^+/Cl^-$  cotransporter (NKCC1) expression and activity that maintains a larger intracellular  $Cl^-$  concentration in astrocytes.

Anenberg et al. [1] found that optogenetic stimulation of GABAergic neurons (inhibitory interneurons) can lead to a net increase in cerebral blood flow (CBF). Whereas Uhlirova et al. [20] found that blood vessels in the brain will only constrict in response to inhibitory nerve cells. They identified NPY as a signal that triggers the constriction of the blood vessels. This signaling molecule is majorly expressed in interneurons and is released by a specific subtype of inhibitory nerve cell. NPY binds to a receptor protein on the SMCs and potentiates vasoconstriction by promoting  $Ca^{2+}$  entry into SMCs via voltage operated  $Ca^{2+}$  channels (VOCCs) [21, 23].

The GABA pathway involves multiple cells:

- **Neuron:**

- GABA opens  $Cl^-$  channels on the neuron, allowing an influx of  $Cl^-$  that hyperpolarises the neuron and inhibits any action potentials [19]

- **Astrocyte:**

- GABA opens  $Cl^-$  channels on the astrocyte, allowing an **efflux** of chlorine that depolarises the astrocyte (the  $Cl^-$  travels out of the cell rather than inwards due to the NKCC1 cotransporter expression and activity that maintains a larger intracellular  $Cl^-$  concentration in astrocytes). Astrocyte depolarisation causes a larger  $K^+$  flux through the big potassium (BK) channel into the PVS  $\rightarrow$  vasodilation [11]

- GABA is recycled through the Krebs cycle to produce glutamate; the glutamate causes an increase in astrocytic  $\text{Ca}^{2+}$  concentration and neuronal NO synthase (nNOS) production → vasodilation [16, 6]

- **SMC:**

- GABA opens  $\text{Cl}^-$  channels on the SMC, allowing an influx of  $\text{Cl}^-$  that hyperpolarises the SMC and closes the VOCCs; hence the  $\text{Ca}^{2+}$  concentration decreases → vasodilation [19]

Whereas the NPY pathway involves only the SMC:

- **SMC:** NPY causes the VOCCs to open, allowing an influx of  $\text{Ca}^{2+}$  into the SMC → **vasoconstriction** [21, 23]

A schematic of these two pathways is shown in Figure 18.

## 2.1 Interneuron Model

In order to model these two pathways we use the NVU model as a base. New equations and parameters are in the Appendix. A schematic of the previous excitatory neuron model is shown in Figure 1 whereas the new interneuron model is shown in Figure 19. The GABA and NPY concentrations are time dependent input functions that can be switched on or off as needed, where during stimulation the concentrations go from zero to some maximal value.

Where the description of models is the same and to provide clarity of reading and to differentiate between the excitatory neuron and interneuron models the important interneuron pathways are coloured in **RED**.

## 2.2 Interneuron model equations and parameters

GABA and NPY are given by time dependent input functions (heaviside functions):

$$GABA_N(t) = \begin{cases} 1 & t_0 < t < t_0 + \Delta t \\ 0 & \text{otherwise} \end{cases} \quad (26)$$

$$NPY_N(t) = \begin{cases} 1 & t_0 < t < t_0 + \Delta t \\ 0 & \text{otherwise} \end{cases} \quad (27)$$

where  $t_0$  is the beginning of stimulation and  $\Delta t$  is the length of stimulation. Note that these GABA and NPY concentrations are nondimensionalised with respect to their maximal values (currently unknown), i.e.  $GABA_N = GABA/GABA_{max}$  so that during the stimulation period  $GABA_N = GABA_{max}/GABA_{max} = 1$  and similarly for NPY.

The GABA dependent  $\text{Cl}^-$  channel fluxes on the astrocyte and SMC are added to the differential equations for  $v_k$  and  $v_i$  respectively and are given by

$$J_{GABA,k} = g_{GABA}(v_k - E_{GABA}) \quad (28)$$

$$J_{GABA,i} = g_{GABA}(v_i - E_{GABA}) \quad (29)$$

where  $v_k$  is the astrocytic membrane potential in mV,  $v_i$  is the SMC membrane potential in mV,  $E_{GABA} = -75$  mV is the reversal potential of the  $\text{Cl}^-$  channels, and the GABA dependent conductance of the channels is given by

$$g_{GABA} = \frac{G_{GABA}}{2} \left( 1 + \tanh \left( \frac{GABA_N - g_{mid}}{g_{slope}} \right) \right) \quad (30)$$

where  $g_{mid} = 0.6$  is the midpoint of the sigmoidal,  $g_{slope}$  is the slope of the sigmoidal (both model estimates), and  $G_{GABA}$  is the maximal conductance of the channel given by  $0.3 \times G_{Cl,i}$  where  $G_{Cl,i} = 1.34 \times 10^{-6} \mu\text{M mV}^{-1} \text{ ms}^{-1}$  is

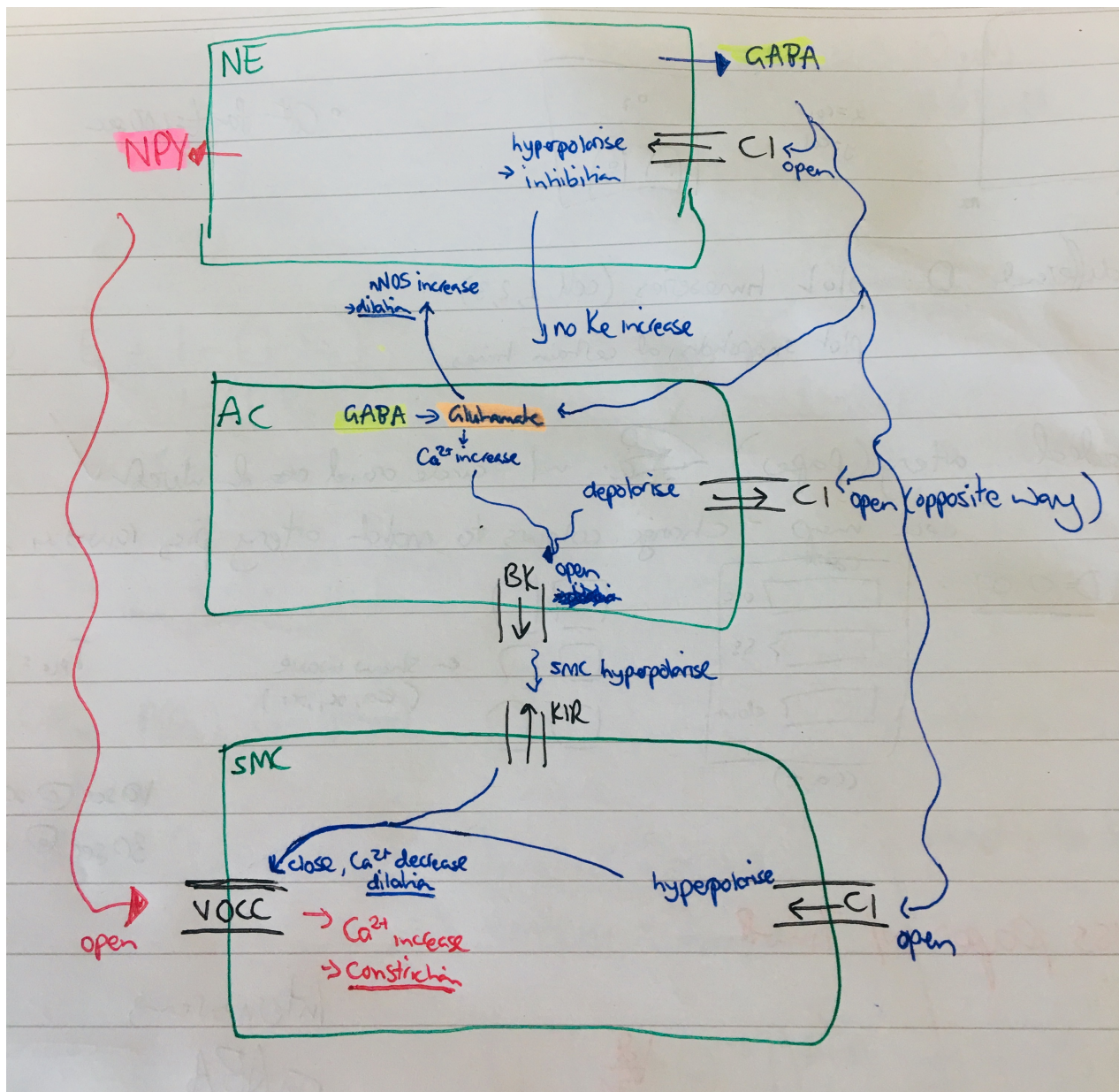


Figure 18: Rough sketch of the GABA and NPY pathways through the neurovascular unit. GABA: vasodilation, NPY: vasoconstriction.

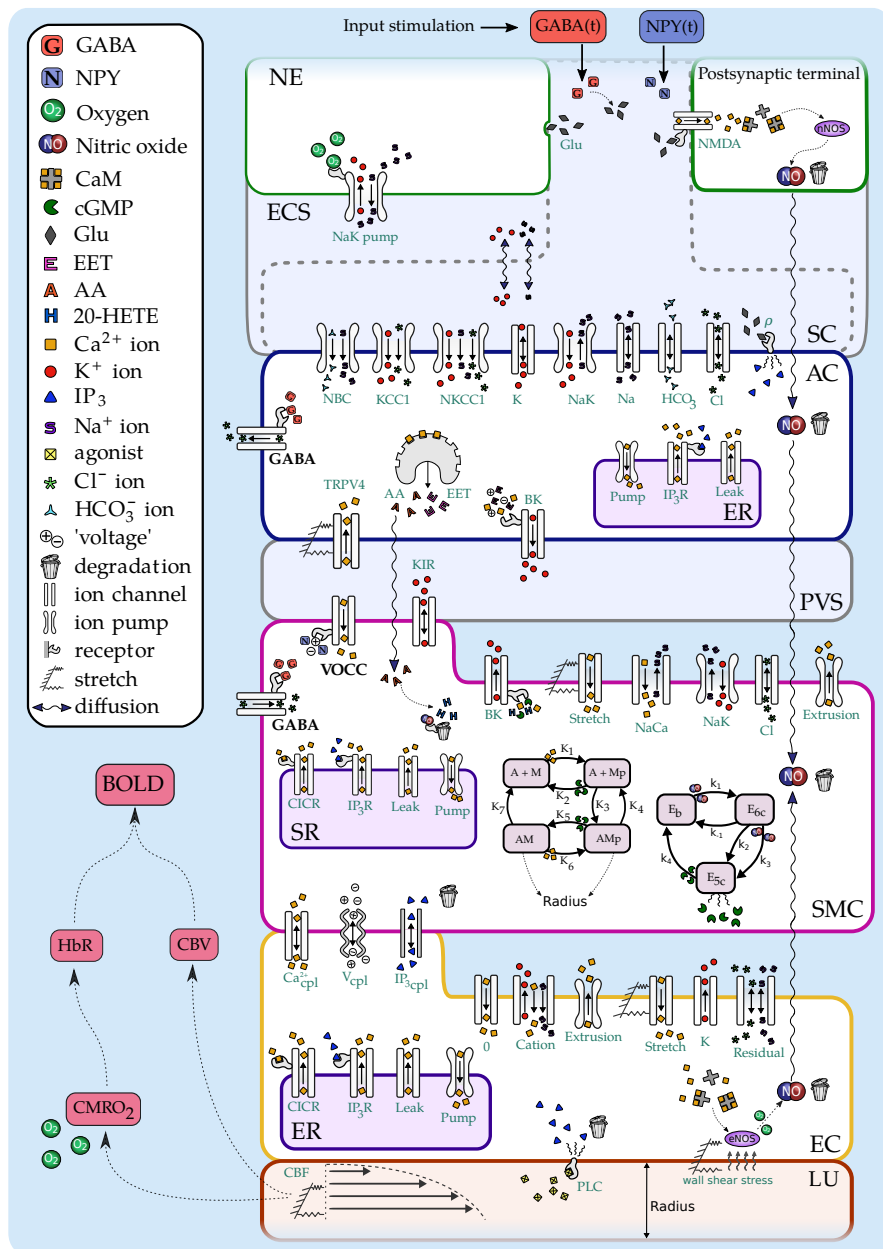


Figure 19: Interneuron model (compare with Figure 1)

the conductance of the SMC  $\text{Cl}^-$  leak channel taken from the NVU model. This is a model estimate and can be changed by fitting to data. Hence when  $GABA_N = 0$ ,  $g_{GABA} = 0$  and when  $GABA_N = 1$ ,  $g_{GABA} = G_{GABA}$ .

The glutamate concentration can either be increased due to neuronal stimulation as in an excitatory neuron (modelled as a glutamate release when extracellular  $\text{K}^+$   $K_e$  is above a threshold  $K_{e_{switch}} = 5.5 \text{ mM}$ ) or increased from production due to GABA. This is modelled by the following equation:

$$Glu = \frac{Glu_{max}}{2} \left( 1 + \tanh \left( \frac{K_e - K_{e_{switch}}}{Glu_{slope}} \right) \right) + \frac{Glu_{max}}{2} \left( 1 + \tanh \left( \frac{GABA_N - g_{mid}}{g_{slope}} \right) \right) \quad (31)$$

where  $Glu_{max} = 1846 \mu\text{M}$  is the maximal glutamate concentration corresponding to a single vesicle release.

Finally the flux of  $\text{Ca}^{2+}$  through the VOCC channel on the SMC is given by

$$J_{VOCC,i} = g_{VOCC} \frac{v_i - v_{Ca1}}{1 + \exp \left( \frac{-(v_i - v_{Ca2})}{R_{Ca}} \right)} \quad (32)$$

where  $v_{Ca1} = 100 \text{ mV}$  is the reversal potential,  $v_{Ca2} = -24 \text{ mV}$  is the half-point of the VOCC activation sigmoidal, and  $R_{Ca} = 8.5 \text{ mV}$  is the maximum slope of the sigmoidal (all taken from the NVU model). The NPY conductance is given by

$$g_{VOCC} = G_{Ca,i} \left( 1 + \frac{N_{inc}}{2} \tanh \left( \frac{NPY_N - N_{mid}}{N_{slope}} \right) \right) \quad (33)$$

where  $G_{Ca,i} = 1.29 \times 10^{-6} \mu\text{M mV}^{-1} \text{ ms}^{-1}$  is the base conductance of the VOCC (taken from the NVU model),  $N_{inc} = 0.05$  is the proportional increase of the conductance from baseline due to NPY (i.e. 0.05 means a 5% increase from  $G_{Ca,i}$  when NPY is released, model estimate),  $N_{mid} = 0.6$  is the midpoint of the sigmoidal, and  $N_{slope}$  is the slope of the sigmoidal (both model estimates). Hence when  $NPY_N = 0$ ,  $g_{VOCC} = G_{Ca,i}$  and when  $NPY_N = 1$ ,  $g_{VOCC} = 1.05 \times G_{Ca,i}$ .

### 3 Equations and Parameters

The following parameters are given for ordinary neurovascular coupling (NVC) conditions.

| Parameter  | Description  | Value                                     |
|------------|--|---|
| $F$        | Faraday's constant                                 | $96.485 \text{ C mmol}^{-1}$              |
| $R_g$      | Gas constant                                       | $8.315 \text{ J mol}^{-1} \text{ K}^{-1}$ |
| $T$        | Temperature constant                               | 300 K                                     |
| $\phi$     | $R_g T / F$ characteristic voltage                 | 26.7 mV                                   |
| $z_K$      | Ionic valence for $\text{K}^+$                     | 1   |
| $z_{Na}$   | Ionic valence for $\text{Na}^+$                    | 1   |
| $z_{Cl}$   | Ionic valence for $\text{Cl}^-$                    | -1  |
| $z_{NBC}$  | Effective valence of the NBC cotransporter complex | -1  |
| $z_{Ca}$   | Ionic valence for $\text{Ca}^{2+}$                 | 2   |
| $\gamma_v$ | Change in membrane potential by a scaling factor   | $1970 \text{ mV } \mu\text{M}^{-1}$       |

### 3.1 Basic Hematology

In order to properly compare with some of the experimental results from both Sheffield (Jason Berwick's group) and others we look at some parameters corresponding to haemoglobin dynamics.

haemoglobin concentration in blood

- Adult Male :-  $135\text{-}175 \text{ gL}^{-1}$
- Adult Female :-  $122\text{-}150 \text{ gL}^{-1}$
- Child :-  $100\text{-}140 \text{ gL}^{-1}$

Molecular weight of haemoglobin =  $64450 \text{ gmol}^{-1}$ .

- Adult Male :-  $2.1\text{-}2.7 \text{ mM}$
- adult Female :-  $1.9\text{-}2.3 \text{ mM}$  Child :-  $1.55\text{-}2.2 \text{ mM}$

haemoglobin ,  $[H]$  decreases from the large arteries to the cerebral vasculature in a ratio of 0.69 (see Wyatt et al 1990, Jour Appl., Physiology, **68**, 1086-1091). With  $[H] = 2.5 \text{ mM}$  in aorta then  $[H]_{\text{brain}} = [H]_b = 2.5 \times 0.69 = 1.725 \text{ mM}$ . Using the Hill equation and a blood saturation of 0.75 we have that

$$[O_2]b = [O_2]_{\text{plasma}} + \frac{[H]bPO}{1 + \frac{\alpha P_{50}}{[O_2]_{\text{plasma}}}} \quad (34)$$

$P_{50} = P_{O_2}$  at which  $[H]$  is 50 % saturated.

(see Valabrague et al , JCBFM, **23**:536-545, 2003). Solving the Hilll equation for  $[O_2]_{\text{plasma}} = 0.053 \text{ mM}$ . (See Hudetz, 1999, Brain Res. **817**:75-83) the ratio of oxygnen concentration in cerebral tissue to plasma is approximately  $0.2 = g$ .

- Average normal CBV: 3.5 %
- Gray Matter : 4.7 %
- White Matter : 2.6 %
- Basal Ganglia : 3.9 %

Hence

- $[HbT]_{\text{tissue}} = 1.725 \text{ mM} \times 3.5\% = 60 \mu M$ .
- Gray Matter  $[HbT]_{\text{tissue}} = 1.725 \text{ mM} \times 4.7\% = 82 \mu M$ .
- Assume  $[HbT]_{\text{tissue}} = 75 \mu M$ .

Here we use the formulation of Buxton for CMRO<sub>2</sub> as the definitions seem to be non-aligned. CMRO<sub>2</sub> is NOT the rate at which the neuron consumes O<sub>2</sub> but the product of the flow in the capillary, the oxygen extraction fraction and the basal oxygen concentration in the precapillary arteriole. In addition the flux  $J_{\text{vasc}}$  is now formed from the oxygen extraction fraction, CBF and the basal oxygen concentration. We define below the new extraction fraction using the analysis of Buxton and Frank and use this in the equations for HbR etc.

#### Extraction fraction

Assumptions

- At rest all brain capillaries are perfused. No capillary recruitment
- All O<sub>2</sub> leaving the capillary are used by the cell's metabolism. i.e. 100 % efficiency
- exchange of O<sub>2</sub> between plasma and RBCs is rapid and hence in equilibrium
- O<sub>2</sub> has a probability k, of being extracted for metabolism. In the simple model k is proportional to the capillary wall permeability P.

Using the above assumptions then defining  $C_p(t)$  as the plasma oxygen concentration,  $C_T(t)$  the total oxygen concentration in the capillary then

$$\frac{dC_T(t)}{dt} = -kC_p(t) \quad (35)$$

with  $C_T(0) = C_a$ . The extraction fraction is defined as

$$E_t(t) = \frac{C_T(0) - C_T(t)}{C_T(0)} \quad (36)$$

Suppose that  $r = \frac{C_p(t)}{C_T(t)} = \text{constant}$  and with all capillaries having the same transit time then the solution to equation (3.1) is ,

$$E = 1 - e^{rkt} \quad (37)$$

Assuming that the volume of the capillary bed remains constant then the characteristic time through the capillary bed is inversely proportional to the flow velocity,  $f_{in} = f$ .

$$\begin{aligned} E_0 &= 1 - e^{rk/f_0} \\ k &= \frac{\ln(1 - E_0)^{f_0}}{r} \\ E(f) &= 1 - (1 - E_0)^{f_0/f} \end{aligned} \quad (38)$$

In this case f is defined to be cerebral blood flow, CBF. However the probability of oxygen crossing the BBB is proportional to the concentration gradient of oxygen in the plasma to that in the cerebral tissue = 0.2, hence we redevelop the Buston extraction fraction equation to include this.

$$\begin{aligned} g &= \frac{[O_2]_{tissue}}{[O_2]_{plasma}} \\ E(f) &= 1 - (1 - E_0)^{\frac{f_0}{f(1-g)}} \end{aligned} \quad (39)$$

In the model we use equation (3.1) since  $E(f_{in})$  defined in equation (3.1) is not unity.

### 3.2 Neuron and Extracellular Space

For the simple neuron model we need to list the inputs to the astrocyte initially to ensure that all required ion concentrations are provided as time-dependent functions. The astrocyte requires concentrations of

- Glutamate
- K<sup>+</sup>
- Na<sup>+</sup>
- HCO<sub>3</sub><sup>-</sup>
- Cl<sup>-</sup>

### 3.3 Input to the model

The input to the neuron model is in two parts. Firstly that of the activation of excitatory neurons ( $E(t)$ ) defined as  $P(t)$  and secondly the activation of inhibitory neurons ( $I(t)$ ) defined as  $Q(t)$ . These are given in the first case as rectangular functions.

$$P(t) = \begin{cases} P_{strength} & \text{for } t_0 \leq t \leq t_f \\ 0 & \text{otherwise} \end{cases} \quad (40)$$

and

$$Q(t) = \begin{cases} Q_{strength} & \text{for } t_0 \leq t \leq t_f \\ 0 & \text{otherwise} \end{cases} \quad (41)$$

### 3.4 ODEs

see Table 4.2 for parameter definitions The membrane potential of the soma/axon ( $v_{sa}$ ) and dendrite ( $v_d$ ) (mV):

$$\frac{dE}{dt} = \frac{1}{\tau_E} \{ -E(t) + (k_e - r_e E(t)) S_e(c_1 E(t) - c_2 I(t) + P(t)) \} \quad (42)$$

$$\frac{dI}{dt} = \frac{1}{\tau_I} \{ -I(t) + (k_i - r_i I(t)) S_i(c_3 E(t) - c_4 I(t) + Q(t)) \} \quad (43)$$

here the functions  $S_e$  and  $S_i$  are given by

$$S_n(x) = \frac{1}{1 + \exp[-a_n(x - \theta_n)]} - \frac{1}{1 + \exp(a_n \theta_n)} \quad n \in e, i \quad (44)$$

$$k_n = \max[S_n(x)] \quad n \in e, i \quad (45)$$

Table 4.2

| Parameter  | Description                                | Value |
|------------|--|-------|
| $a_e$      | sigmoid coefficient                        | 1.2   |
| $\theta_e$ | sigmoid coefficient                        | 2.8   |
| $\tau_e$   | characteristic time for excitatory neurons | 3 ms  |
| $a_i$      | sigmoid coefficient                        | 1.0   |
| $\theta_i$ | sigmoid coefficient                        | 4.0   |
| $\tau_i$   | characteristic time for inhibitory neurons | 3 ms  |
| $r_e$      | coefficient                                | 1     |
| $r_i$      | coefficient                                | 1     |
| $c_1$      | coefficient                                | 12    |
| $c_2$      | coefficient                                | 10    |
| $c_3$      | coefficient                                | 13    |
| $c_4$      | coefficient                                | 11    |

Table 2: Nominal parameters of the neuron populations.

We should note here that the nominal parameters given in Table 4.2 could change depending on the experimental stimulation. This variation has yet to be fully investigated and described. To find the value of  $k_{e,i}$  we use  $x = 10$  such

that  $k_n = S_n(x)$  and this gives a maximum value.

The K<sup>+</sup> in the extracellular space (ECS) and Na<sup>+</sup> ion concentrations in the soma and dendrite (mM):

$$\frac{dNa_{sa}}{dt} = -\beta_{Na_{sa}}(Na_{sa} - Na_{sabase}) + \alpha_{Na_{sa}}\beta_{Na_{sa}} \frac{[| E(t) - I(t) |]}{EI_0} \quad (46)$$

$$\frac{dNa_d}{dt} = -\beta_{Na_d}(Na_d - Na_{dbase}) + \alpha_{Na_d}\beta_{Na_d} \frac{[| E(t) - I(t) |]}{EI_0} \quad (47)$$

$$\frac{dK_e}{dt} = -\beta_{Ke}(K_e - K_{base}) + \alpha_{Ke}\beta_{Ke} \frac{[| E(t) - I(t) |]}{EI_0} \quad (48)$$

Table 3.4

| Parameter          | Description | Value               |
|--------------------|-------------|---------------------|
| $\alpha_{Ke}$      |             | 2.1 (this can vary) |
| $\beta_{Ke}$       |             | 4.2e-3              |
| $\alpha_{Na_{sa}}$ |             | 4.23                |
| $\beta_{Na_{sa}}$  |             | 0.39e-3             |
| $\alpha_{Na_d}$    |             | -2.12               |
| $\beta_{Na_d}$     |             | 0.75e-3             |
| $K_{base}$         |             | 3.5                 |
| $Na_{sabase}$      |             | 9.37                |
| $Na_{dbase}$       |             | 9.42                |

Table 3: Nominal parameters of the neuron populations.

AGAIN we should note here that the nominal parameters given in Table 3.4 could change depending on the experimental stimulation. This variation has yet to be fully investigated and described.

### 3.5 Algebraic Variables

The oxygen consumption ode is the same as the old Kager neuron model.

$$\frac{dO_2}{dt} = J_{O_2 \text{vascular}} - J_{O_2 \text{background}} - J_{O_2 \text{pump}} \quad (49)$$

In the full model this PUMP is defined as  $J_{O_2 \text{pump}}$  which is function of the ECS K<sup>+</sup> and the soma or dendrite concentration of Na<sup>+</sup>. This works for the new model as all we need to know is the concentrations of ECS K<sup>+</sup> and the soma or dendrite concentration of Na<sup>+</sup> and we have that from the solution of the 'simple' odes.

The cerebral blood flow (-):(assuming Poiseuille Flow)

$$\text{CBF} = \text{CBF}_{init} \frac{R^4}{R_{init}^4} \quad (50)$$

The vascular supply of oxygen (mM s<sup>-1</sup>) is defined by the amount of oxygen extracted and passed across the blood brain barrier, since CBF is defined in terms of mM s<sup>-1</sup>:

$$J_{O_2 \text{ vascular}} = \text{CBF} \frac{E(t)}{E_0} \quad (51)$$

The background oxygen consumption ( $\text{mM s}^{-1}$ ):

$$J_{O_2 \text{ background}} = J_0 P_{O_2} (1 - \gamma_{O_2}) \quad (52)$$

The normalised pump rate (-):

$$P_{O_2} = \frac{J_{\text{pump2}}(O_2) - J_{\text{pump2}}(0)}{J_{\text{pump2}}(O_2_o) - J_{\text{pump2}}(0)} \quad (53)$$

We can simplify this considerably

$$\begin{aligned} J_{\text{pump2}}(O_2) &= 2 \left[ 1 + \frac{O_2_o}{(1 - \alpha_{O_2})O_2 + \alpha_{O_2}O_2_o} \right]^{-1} \\ J_{\text{pump2}}(O_2_o) &= 1 \\ J_{\text{pump2}}(0) &= 2 \left[ 1 + \frac{1}{\alpha_{O_2}} \right]^{-1} = \frac{2\alpha_{O_2}}{1 + \alpha_{O_2}} \end{aligned} \quad (54)$$

so

$$\begin{aligned} J_{\text{pump2}}(O_2_o) - J_{\text{pump2}}(0) &= 1 - \frac{2\alpha_{O_2}}{1 + \alpha_{O_2}} \\ &= \frac{1 - \alpha_{O_2}}{1 + \alpha_{O_2}} \end{aligned} \quad (55)$$

hence the nomalised pump rate is evaluated as

$$\begin{aligned} P_{O_2} &= \frac{J_{\text{pump2}}(O_2) - \frac{2\alpha_{O_2}}{1 + \alpha_{O_2}}}{\frac{1 - \alpha_{O_2}}{1 + \alpha_{O_2}}} \\ &= \frac{(1 + \alpha_{O_2})J_{\text{pump2}}(O_2) - 2\alpha_{O_2}}{1 - \alpha_{O_2}} \end{aligned} \quad (56)$$

## 4 BOLD response

### 4.1 ODEs

The non dimensional cerebral blood volume (CBV) (-):

$$\frac{d\text{CBV}}{dt} = \frac{1}{\tau_{MTT} + \tau_{TAT}} \left( f_{in} - \text{CBV}^{\frac{1}{d}} \right) \quad (57)$$

with  $f_{in} = \frac{CBF}{CBF_{init}}$

The non dimensional deoxyhemoglobin (HbR) concentration (-):

$$\frac{d\text{HbR}}{dt} = \frac{1}{\tau_{MTT}} \left( \frac{f_{in}E(t)}{E_0} - \frac{\text{HbR}}{\text{CBV}} f_{out} \right) \quad (58)$$

$$f_{out} = \text{CBV}^{\frac{1}{d}} + \tau_{TAT} \frac{d\text{CBV}}{dt} \quad (59)$$

Here  $f_{out}$  is the flow out of the venous balloon.

## 4.2 Algebraic Variables

The non dimensional normalised total hemoglobin (HbT) concentration (-):

$$\text{HbR}_N = \frac{\text{HbR}_N}{\text{HbR}(0)} \quad (60)$$

$$\text{HbT}_N = \frac{\text{CBF}_N \text{HbR}_N}{\text{CMRO}_{2_N}} \quad (61)$$

where the normalised CBF is given by  $\text{CBF}_N = \text{CBF}/\text{CBF}(0)$  and  $\text{CBF}(0)$  is the steady state value, similarly for HbR.  $\text{CMRO}_2 = f_{in} \frac{E(t)}{E_0}$  and  $\text{CMRO}_2 0 = 1$ , hence

$$\begin{aligned} \text{HbT}_N &= \text{CBF}_N \text{HbR}_N \frac{E_0}{f_{in} E(t)} \\ &= \text{HbR} \frac{E_0}{E(t)} \end{aligned} \quad (62)$$

The non dimensional normalised oxyhemoglobin (HbO) concentration (-):

$$\text{HbO}_N = \text{HbT}_N - \text{HbR}_N + 1 \quad (63)$$

The BOLD signal change from its steady state value (-):

$$\Delta \text{BOLD} \approx V_0 (a_1 [1 - \text{HbR}_N] + a_2 [\text{CBV}_N - 1]) \quad (64)$$

| Parameter    | Description                            | Value |
|--------------|--|-------|
| $\tau_{MTT}$ | Mean transit time                      | 3 s   |
| $\tau_{TAT}$ | Transient adjustment time constant     | 20 s  |
| $d$          | Empirical relation between CBF and CBV | 2.5   |
| $a_1$        | Weight for HbR change                  | 3.4   |
| $a_2$        | Weight for CBV change                  | 1     |
| $V_0$        | Resting venous blood volume fraction   | 0.03  |
| $E_0$        | Baseline oxygen extraction fraction    | 0.4   |

Table 4: Parameters of the BOLD submodel, for references see Mathias et al. [13].

| Parameter           | Description  | Value                    |
|---------------------|--|--------------------------|
| $t_0$               | Start time of input current                              | 0 s                      |
| $t_f$               | Final time of input current                              | variable                 |
| $O_2 0$             | Equilibrium tissue oxygen level                          | 0.01 mM                  |
| $\gamma_{O2}$       | Fraction of the total oxygen consumption at steady state | 0.1                      |
| $J_0$               | Equilibrium change in oxygen concentration due to CBF    | 0.053 mM s <sup>-1</sup> |
| $\text{CBF}_{init}$ | Equilibrium CBF  | 0.032                    |
| $J_{pump1s_{a_0}}$  | Steady state pump rate in the soma/axon                  | 0.0312                   |
| $J_{pump1d_0}$      | Steady state pump rate in the dendrite                   | 0.0312                   |
| $R_{init}$          | Vessel radius when passive and no stress is applied      | 20 $\mu\text{m}$         |

|                   |  |                           |
|-------------------|--|---------------------------|
| $\alpha_{O2}$     | Fraction of oxygen independent adenosine triphosphate (ATP) production | 0.05                      |
| $J_{pump2}(0)$    | Pump rate when oxygen concentration is 0                               | 0.0952                    |
| $J_{pump2}(O2_0)$ | Pump rate when oxygen is at equilibrium                                | 1                         |
| $K_{e,0}$         | Equilibrium $K_e$  | 2.9 mM                    |
| $Na_{sa,0}$       | Equilibrium $Na_{sa}$  | 10 mM                     |
| $Na_{d,0}$        | Equilibrium $Na_d$   | 10 mM                     |
| $I_{max}$         | Maximum rate of $Na^+/K^+$ ATP-ase pump                                | 0.078 mA cm <sup>-2</sup> |

Table 5: Parameters of the neuron and extracellular space submodel, for references see Mathias et al. [13].

## 5 Synaptic Cleft and Astrocyte

### 5.1 ODEs

$K^+$  concentration in the synaptic cleft (SC) ( $\mu\text{M}$ ):

$$\frac{dK_s}{dt} = \frac{1}{VR_{sk}} (J_{K_k} - 2J_{NaK_k} - J_{NKCC1_k} - J_{KCC1_k}) + J_{KNEtoSC} \quad (65)$$

$Na^+$  concentration in the SC ( $\mu\text{M}$ ):

$$\frac{dNa_s}{dt} = \frac{1}{VR_{sk}} (J_{Na_k} + 3 * J_{NaK_k} - J_{NKCC1_k} - J_{NBC_k}) - J_{NaNEtoSC} \quad (66)$$

$HCO_3^-$  concentration in the SC ( $\mu\text{M}$ ):

$$\frac{dHCO_{3s}}{dt} = \frac{1}{VR_{sk}} (-2J_{NBC_k}) \quad (67)$$

$K^+$  concentration in the astrocyte ( $\mu\text{M}$ ):

$$\frac{dK_k}{dt} = -J_{K_k} + 2J_{NaK_k} + J_{NKCC1_k} + J_{KCC1_k} - J_{BK_k} \quad (68)$$

$Na^+$  concentration in the astrocyte ( $\mu\text{M}$ ):

$$\frac{dNa_k}{dt} = -J_{Na_k} - 3J_{NaK_k} + J_{NKCC1_k} + J_{NBC_k} \quad (69)$$

$HCO_3^-$  concentration in the astrocyte ( $\mu\text{M}$ ):

$$\frac{dHCO_{3k}}{dt} = 2J_{NBC_k} \quad (70)$$

$Cl^-$  concentration in the astrocyte via electroneutrality ( $\mu\text{M}$ ):

$$\frac{dCl_k}{dt} = \frac{dNa_k}{dt} + \frac{dK_k}{dt} - \frac{dHCO_{3k}}{dt} + 2\frac{dCa_k}{dt} \quad (71)$$

The astrocytic cytosolic  $Ca^{2+}$  concentration ( $\mu\text{M}$ ):

$$\frac{dCa_k}{dt} = B_{cyt} \left( J_{IP3_k} - J_{pump_k} + J_{ERleak_k} - \frac{J_{TRPV_k}}{r_{buff}} \right) \quad (72)$$

The astrocytic inositol trisphosphate ( $IP_3$ ) concentration ( $\mu\text{M}$ ):

$$\frac{dIP3_k}{dt} = r_h G - k_{deg} IP3_k \quad (73)$$

The astrocytic epoxyeicosatrienoic acid (EET) concentration ( $\mu\text{M}$ ):

$$\frac{deet_k}{dt} = V_{eet} \max(Ca_k - c_{k_{min}}, 0) - k_{eet} eet_k \quad (74)$$

The  $\text{Ca}^{2+}$  concentration in the astrocytic endoplasmic reticulum (ER) ( $\mu\text{M}$ ):

$$\frac{ds_k}{dt} = \frac{-B_{cyt}}{VR_{ERcyt}} (J_{IP3_k} - J_{pump_k} + J_{ERleak_k}) \quad (75)$$

Membrane potential of the astrocyte (AC) (mV):

$$\frac{dv_k}{dt} = \gamma_v (-J_{BK_k} - J_{K_k} - J_{Cl_k} - J_{NHC_k} - J_{Na_k} - J_{NaK_k} - 2J_{TRPV_k} - J_{GABA,k}) \quad (76)$$

The open probability of the BK channel (-):

$$\frac{dw_k}{dt} = \phi_n(w_\infty - w_k) \quad (77)$$

The inactivation variable  $h_k$  of the astrocytic  $IP_3R$  channel (-):

$$\frac{dh_k}{dt} = k_{on} [K_{inh} - (Ca_k + K_{inh})h_k] \quad (78)$$

The concentration of arachidonic acid in the astrocyte  $AA_k$ .

$$\frac{dAA_k}{dt} = \frac{AA_m AA_{max}}{(AA_m + (Ca_k - Ca_0))^2 \frac{dCa_k}{dt}} + \frac{(AA_i - AA_k)}{\tau_{AA}} \quad (79)$$

$$\tau_{AA} = \frac{x_{ki}^2}{2D_{AA}} \quad (80)$$

## 5.2 Algebraic Variables

The glutamate concentration in the SC ( $\mu\text{M}$ ):

$$Glu = \frac{Glu_{max}}{2} \left( 1 + \tanh \left( \frac{K_e - Ke_{switch}}{Glu_{slope}} \right) \right) + \frac{Glu_{max}}{2} \left( 1 + \tanh \left( \frac{GABA_N - g_{mid}}{g_{slope}} \right) \right) \quad (81)$$

$$J_{GABA,k} = g_{GABA}(v_k - E_{GABA}) \quad (82)$$

$$g_{GABA} = \frac{G_{GABA}}{2} \left( 1 + \tanh \left( \frac{GABA_N - g_{mid}}{g_{slope}} \right) \right) \quad (83)$$

$G_{GABA}$  is the maximal conductance of the channel given by  $0.3 \times G_{Cl,i}$  where  $G_{Cl,i} = 1.34 \times 10^{-6} \mu\text{M mV}^{-1} \text{ ms}^{-1}$  is the conductance of the SMC  $\text{Cl}^-$  leak channel taken from the excitatory NWU model (i.e. Wilson Cowan).

The flux of  $\text{K}^+$  into the SC based on the extracellular  $\text{K}^+$  ( $\mu\text{Ms}^{-1}$ ):

$$J_{KNEtoSC} = J_{NaNetoSC} = c_{unit} k_{syn} \frac{dK_e}{dt} \quad (84)$$

$\text{Cl}^-$  concentration in the SC via electroneutrality ( $\mu\text{M}$ ):

$$Cl_s = Na_s + K_s - HCO_3_s \quad (85)$$

$\text{Cl}^-$  flux through the  $\text{Cl}^-$  channel ( $\mu\text{M s}^{-1}$ ):

$$J_{Cl_k} = G_{Cl_k}(v_k - E_{Cl_k}) \quad (86)$$

$\text{K}^+$  flux through the  $\text{K}^+$  channel ( $\mu\text{M s}^{-1}$ ):

$$J_{K_k} = G_{K_k}(v_k - E_{K_k}) \quad (87)$$

$\text{Na}^+$  flux through the  $\text{Na}^+$  channel ( $\mu\text{M s}^{-1}$ ):

$$J_{Na_k} = G_{Na_k}(v_k - E_{Na_k}) \quad (88)$$

$\text{Na}^+$  and  $\text{HCO}_3^-$  flux through the NBC channel ( $\mu\text{M s}^{-1}$ ):

$$J_{NBC_k} = G_{NBC_k}(v_k - E_{NBC_k}) \quad (89)$$

$\text{Cl}^-$  and  $\text{K}^+$  flux through the KCC1 channel ( $\mu\text{M s}^{-1}$ ):

$$J_{KCC1_k} = G_{KCC1_k}\phi \ln\left(\frac{K_s Cl_s}{K_k Cl_k}\right) \quad (90)$$

$\text{Na}^+$ ,  $\text{K}^+$  and  $\text{Cl}^-$  flux through the NKCC1 channel ( $\mu\text{M s}^{-1}$ ):

$$J_{NKCC1_k} = G_{NKCC1_k}\phi \ln\left(\frac{Na_s K_s Cl_s^2}{Na_k K_k Cl_k^2}\right) \quad (91)$$

Flux through the  $\text{Na}^+/\text{K}^+$  ATP-ase pump ( $\mu\text{M s}^{-1}$ ):

$$J_{NaK_k} = J_{NaK_{max}} \frac{Na_k^{1.5}}{Na_k^{1.5} + K_{Na_k}^{1.5}} \frac{K_s}{K_s + K_{K_s}} \quad (92)$$

$\text{K}^+$  flux through the BK channel ( $\mu\text{M s}^{-1}$ ):

$$J_{BK_k} = G_{BK_k} w_k (v_k - E_{BK_k}) \quad (93)$$

Nernst potential for the  $\text{K}^+$  channel (mV):

$$E_{K_k} = \frac{\phi}{z_K} \ln\left(\frac{K_s}{K_k}\right) \quad (94)$$

Nernst potential for the  $\text{Na}^+$  channel (mV):

$$E_{Na_k} = \frac{\phi}{z_{Na}} \ln\left(\frac{Na_s}{Na_k}\right) \quad (95)$$

Nernst potential for the  $\text{Cl}^-$  channel (mV):

$$E_{Cl_k} = \frac{\phi}{z_{Cl}} \ln\left(\frac{Cl_s}{Cl_k}\right) \quad (96)$$

Nernst potential for the NBC channel (mV):

$$E_{NBC_k} = \frac{\phi}{z_{NBC}} \ln\left(\frac{Na_s HCO_{3_s}^2}{Na_k HCO_{3_k}^2}\right) \quad (97)$$

Nernst potential for the BK channel (mV):

$$E_{BK_k} = \frac{\phi}{z_K} \ln\left(\frac{K_p}{K_k}\right) \quad (98)$$

The time constant associated with the opening of the BK channel ( $\text{s}^{-1}$ ):

$$\phi_n = \psi_n \cosh\left(\frac{v_k - v_3}{2v_4}\right) \quad (99)$$

The equilibrium state of the BK channel (-):

$$w_\infty = \frac{1}{2} \left( 1 + \tanh\left(\frac{v_k + eet_{shift}eet_k - v_3}{v_4}\right) \right) \quad (100)$$

The voltage associated with half open probability (mV):

$$v_3 = -\frac{v_5}{2} \tanh\left(\frac{Ca_k - Ca_3}{Ca_4}\right) + v_6 \quad (101)$$

The ratio  $\rho$  of bound to unbound metabotropic receptors on the astrocytic process adjacent to the SC (-):

$$\rho = \rho_{\min} + \frac{\rho_{\max} - \rho_{\min}}{Glu_{\max}} Glu \quad (102)$$

The ratio  $G$  of active to total G-protein due to metabotropic glutamate receptor (mGluR) binding on the astrocyte endfoot surround the SC (-):

$$G = \frac{\rho + \delta_G}{K_G + \rho + \delta_G} \quad (103)$$

Fast  $\text{Ca}^{2+}$  buffering in the astrocytic cytosol is described within the steady state approximation (-):

$$B_{cyt} = \left( 1 + BK_{end} + \frac{K_{ex}B_{ex}}{(K_{ex} + Ca_k)^2} \right)^{-1} \quad (104)$$

The flux of  $\text{Ca}^{2+}$  through the IP<sub>3</sub>R channel ( $\mu\text{M s}^{-1}$ ):

$$J_{IP3_k} = J_{max} \left[ \left( \frac{IP3_k}{IP3_k + K_i} \right) \left( \frac{Ca_k}{Ca_k + K_{act_k}} \right) h_k \right]^3 \left( 1 - \frac{Ca_k}{s_k} \right) \quad (105)$$

The flux of  $\text{Ca}^{2+}$  through the uptake pump ( $\mu\text{M s}^{-1}$ ):

$$J_{pump_k} = V_{max} \frac{Ca_k^2}{Ca_k^2 + k_{pump}^2} \quad (106)$$

The flux of  $\text{Ca}^{2+}$  through the leak channel ( $\mu\text{M s}^{-1}$ ):

$$J_{ERleak_k} = P_L \left( 1 - \frac{Ca_k}{s_k} \right) \quad (107)$$

| Parameter        | Description  | Value  |
|------------------|--|--|
| $VR_{sk}$        | Volume ratio between the SC and astrocyte            | 0.465  |
| $Glu_{max}$      | Maximum glutamate concentration (one vesicle)        | $1846 \mu\text{M}$                           |
| $K_{e_{switch}}$ | Threshold past which glutamate is released           | 5.0 mM                                       |
| $Glu_{slope}$    | Slope of glutamate sigmoidal                         | 0.1 mM                                       |
| $c_{unit}$       | Constant to convert from mM to $\mu\text{M}$         | $10^3$                                       |
| $k_{syn}$        | The number of active synapses per astrocytic process | 11.5   |
| $G_{K_k}$        | Whole cell conductance of $\text{K}^+$               | $6907.77 \mu\text{M mV}^{-1} \text{ s}^{-1}$ |
| $G_{Na_k}$       | Whole cell conductance of $\text{Na}^+$              | $226.94 \mu\text{M mV}^{-1} \text{ s}^{-1}$  |
| $G_{NBC_k}$      | Whole cell conductance of the NBC cotransporter      | $130.74 \mu\text{M mV}^{-1} \text{ s}^{-1}$  |
| $G_{KCC1_k}$     | Whole cell conductance of the KCC1 cotransporter     | $1.728 \mu\text{M mV}^{-1} \text{ s}^{-1}$   |

|                 |   |   |
|-----------------|---|---|
| $G_{NKCC1_k}$   | Whole cell conductance of the NKCC1 cotransporter   | $9.568 \mu\text{M mV}^{-1} \text{ s}^{-1}$  |
| $G_{BK_k}$      | Whole cell conductance of the BK channel  | $10.25 \mu\text{M mV}^{-1} \text{ s}^{-1}$  |
| $G_{Cl_k}$      | Whole cell conductance of $\text{Cl}^-$   | $151.93 \mu\text{M mV}^{-1} \text{ s}^{-1}$ |
| $J_{NaK_{max}}$ | Maximum flux through the $\text{Na}^+/\text{K}^+$ ATP-ase pump                                  | $2.37 \times 10^4 \mu\text{M s}^{-1}$       |
| $K_{Na_k}$      | $\text{Na}^+/\text{K}^+$ ATP-ase pump constant  | $10 \times 10^3 \mu\text{M}$                |
| $K_{K_s}$       | $\text{Na}^+/\text{K}^+$ ATP-ase pump constant  | $1.5 \times 10^3 \mu\text{M}$               |
| $\rho_{\min}$   | Minimum ratio of bound to unbound $\text{IP}_3$ receptors                                       | 0.1   |
| $\rho_{\max}$   | Maximum ratio of bound to unbound $\text{IP}_3$ receptors                                       | 0.7   |
| $\delta_G$      | Ratio of the activities of the unbound and bound receptors                                      | $1.235 \times 10^{-2}$                      |
| $K_G$           | G-protein disassociation constant   | 8.82  |
| $r_h$           | Maximum rate of $\text{IP}_3$ production in astrocyte due to glutamate receptors                | $4.8 \mu\text{M s}^{-1}$                    |
| $k_{deg}$       | Rate constant for $\text{IP}_3$ degradation in astrocyte  | $1.25 \text{ s}^{-1}$                       |
| $r_{buf}$       | Rate of $\text{Ca}^{2+}$ buffering at the endfoot compared to the astrocyte body                | 0.05  |
| $VR_{ERcyt}$    | Volume ratio between ER and astrocytic cytosol  | 0.185                                       |
| $BK_{end}$      | Ratio of endogenous buffer concentration to disassociation constant                             | 40  |
| $K_{ex}$        | Disassociation constant of exogenous buffer   | $0.26 \mu\text{M}$                          |
| $B_{ex}$        | Concentration of exogenous buffer   | $11.35 \mu\text{M}$                         |
| $J_{max}$       | Maximum rate of $\text{Ca}^{2+}$ through the $\text{IP}_3$ mediated channel                     | $2880 \mu\text{M s}^{-1}$                   |
| $K_i$           | Disassociation constant for $\text{IP}_3$ binding to an $\text{IP}_3R$                          | $0.03 \mu\text{M}$                          |
| $K_{act_k}$     | Disassociation constant for $\text{Ca}^{2+}$ binding to an activation site on an $\text{IP}_3R$ | $0.17 \mu\text{M}$                          |
| $k_{on}$        | Rate of $\text{Ca}^{2+}$ binding to the inhibitory site on the $\text{IP}_3R$                   | $2 \mu\text{M}^{-1} \text{ s}^{-1}$         |
| $K_{inh}$       | Disassociation constant of $\text{IP}_3R$   | $0.1 \mu\text{M}$                           |
| $V_{max}$       | Maximum rate of $\text{Ca}^{2+}$ uptake pump on the ER  | $20 \mu\text{M s}^{-1}$                     |
| $k_{pump}$      | $\text{Ca}^{2+}$ uptake pump disassociation constant  | $0.24 \mu\text{M}$                          |
| $P_L$           | ER leak channel steady state balance constant   | $0.0804 \mu\text{M s}^{-1}$                 |
| $V_{eet}$       | EET production rate   | $72 \text{ s}^{-1}$                         |
| $c_{k_{min}}$   | Minimum $\text{Ca}^{2+}$ concentration required for EET production                              | $0.1 \mu\text{M}$                           |
| $k_{eet}$       | EET degradation rate  | $7.2 \text{ s}^{-1}$                        |
| $v_4$           | Measure of the spread of $w_\infty$   | 8 mV  |
| $eet_{shift}$   | Describes the EET dependent voltage shift   | $2 \text{ mV } \mu\text{M}^{-1}$            |
| $v_5$           | Determines the range of the shift of $w_\infty$ as $\text{Ca}^{2+}$ varies                      | 15 mV                                       |
| $v_6$           | Shifts the range of $w_\infty$  | -55 mV                                      |
| $\psi_n$        | Characteristic time for the opening of the BK channel   | $2.664 \text{ s}^{-1}$                      |
| $Ca_3$          | BK open probability $\text{Ca}^{2+}$ constant   | $0.4 \mu\text{M}$                           |
| $Ca_4$          | BK open probability $\text{Ca}^{2+}$ constant   | $0.35 \mu\text{M}$                          |
| $AA_m$          | dissociation constant for $AA_k$  | $0.161 \mu\text{M}$                         |
| $AA_{max}$      | maximum rate of generation of $AA_k$  | $29 \mu\text{M s}^{-1}$                     |
| $Ca_0$          | baseline $\text{Ca}_k^{2+}$   | $0.1432 \mu\text{M}$                        |
| $D_{AA}$        | diffusion coefficient for AA  | $0.152 \mu\text{m}^2 \text{ ms}^{-1}$       |
| $EGABA$         | Nernst potential for GABA   | -75 mV                                      |
| $g_{mid}$       | midpoint of the GABA sigmoidal  | 0.6   |
| $g_{slope}$     | scaling for the GABA sigmoidal  | 0.1   |

Table 6: Parameters of the astrocyte and SC submodel, for references see Dormanns et al. [3], Kenny et al. [8].

## 6 PVS

### 6.1 ODEs

$K^+$  concentration in the PVS ( $\mu M$ ):

$$\frac{dK_p}{dt} = \frac{J_{BK_k}}{VR_{pk}} + \frac{J_{KIR_i}}{VR_{pi}} - K_{decay_p}(K_p - K_{min_p}) \quad (108)$$

$Ca^{2+}$  concentration in the PVS ( $\mu M$ ):

$$\frac{dCa_p}{dt} = \frac{J_{TRPV_k}}{VR_{pk}} + \frac{J_{VOCC_i}}{VR_{pi}} - Ca_{decay_p}(Ca_p - Ca_{min_p}) \quad (109)$$

The open probability of the transient receptor potential vannilloid-related 4 (TRPV4) channel (-):

$$\frac{dm_k}{dt} = \frac{m_{\infty_k} - m_k}{t_{TRPV_k}} \quad (110)$$

### 6.2 Algebraic Variables

The flux of  $Ca^{2+}$  through the VOCC which connects the SMC to the PVS ( $\mu M s^{-1}$ ):

$$J_{VOCC_i} = G_{Cai} \frac{v_i - v_{Ca1}}{1 + \exp[-(v_i - v_{Ca2})/R_{Cai}]} \quad (111)$$

This VOCC channel is altered when the interneuron model is used. See below equation (148)

The flux of  $Ca^{2+}$  through the TRPV4 channel ( $\mu M s^{-1}$ ):

$$J_{TRPV_k} = G_{TRPV_k} m_k (v_k - E_{TRPV_k}) \quad (112)$$

The Nernst potential of the TRPV4 channel (mV):

$$E_{TRPV_k} = \frac{\phi}{z_{Ca}} \ln \left( \frac{Ca_p}{Ca_k} \right) \quad (113)$$

The equilibrium state of the TRPV4 channel (-):

$$m_{\infty_k} = \Gamma_m \left[ \frac{1}{1 + H_{Ca_k}} \left( H_{Ca_k} + \tanh \left( \frac{v_k - v_{1,TRPV}}{v_{2,TRPV}} \right) \right) \right] \quad (114)$$

The material strain gating term (-):

$$\Gamma_m = \frac{1}{1 + \exp \left( -\frac{\eta - \eta_0}{\kappa_k} \right)} \quad (115)$$

The strain on the perivascular endfoot of the astrocyte (-)

$$\eta = \frac{R - R_{init}}{R_{init}} \quad (116)$$

The  $Ca^{2+}$  inhibitory term (-)

$$H_{Ca_k} = \frac{Ca_k}{\gamma_{Cai}} + \frac{Ca_p}{\gamma_{Cae}} \quad (117)$$

| Parameter       | Description  | Value  |
|-----------------|--|--|
| $VR_{pk}$       | Volume ratio between PVS and astrocyte                   | 0.001  |
| $VR_{pi}$       | Volume ratio between PVS and SMC                         | 0.001  |
| $K_{decay_p}$   | Rate of decay of $K^+$ in PVS                            | $0.15 \text{ s}^{-1}$                                    |
| $K_{min_p}$     | Steady state value of $K^+$ in PVS                       | $3 \times 10^3 \mu\text{M}$                              |
| $C_{decay_p}$   | Rate of decay of $\text{Ca}^{2+}$ in PVS                 | $0.5 \text{ s}^{-1}$                                     |
| $C_{a_{min_p}}$ | Steady state value of $\text{Ca}^{2+}$ in PVS            | $2 \times 10^3 \mu\text{M}$                              |
| $G_{Cai}$       | VOCC whole cell conductance                              | $1.29 \times 10^{-3} \mu\text{M mV}^{-1} \text{ s}^{-1}$ |
| $v_{Ca1}$       | VOCC reversal potential                                  | 100 mV   |
| $v_{Ca2}$       | Half point of the VOCC activation sigmoidal              | -24 mV   |
| $R_{Cai}$       | Maximum slope of the VOCC activation sigmoidal           | 8.5 mV   |
| $G_{TRPV_k}$    | TRPV4 whole cell conductance                             | $3.15 \times 10^{-4} \mu\text{M mV}^{-1} \text{ s}^{-1}$ |
| $t_{TRPV_k}$    | Characteristic time constant for $m_k$                   | 0.9 s  |
| $\eta_0$        | Strain required for half activation of the TRPV4 channel | 0.1  |
| $\kappa_k$      | TRPV4 channel strain constant                            | 0.1  |
| $v_{1,TRPV}$    | TRPV4 channel voltage gating constant                    | 120 mV   |
| $v_{2,TRPV}$    | TRPV4 channel voltage gating constant                    | 13 mV  |
| $\gamma_{Cai}$  | $\text{Ca}^{2+}$ concentration constant                  | 0.01 $\mu\text{M}$                                       |
| $\gamma_{Cae}$  | $\text{Ca}^{2+}$ concentration constant                  | 200 $\mu\text{M}$  |

Table 7: Parameters of the PVS compartment, for references see Dormanns et al. [3], Kenny et al. [8].

## 7 SMC

### 7.1 ODEs

Cytosolic  $\text{Ca}^{2+}$  in the SMC ( $\mu\text{M}$ ):

$$\begin{aligned} \frac{dC_{ai}}{dt} = & J_{IP_{3i}} - J_{SR_{uptake_i}} + J_{CICR_i} - J_{extrusion_i} + J_{SR_{leak_i}} \dots \\ & - J_{VOCC_i} + J_{Na/Ca_i} - 0.1J_{stretch_i} + J_{Ca^{2+}-coupling_i}^{SMC-EC} \end{aligned} \quad (118)$$

$\text{Ca}^{2+}$  in the sarcoplasmic reticulum (SR) of the SMC ( $\mu\text{M}$ ):

$$\frac{ds_i}{dt} = J_{SR_{uptake_i}} - J_{CICR_i} - J_{SR_{leak_i}} \quad (119)$$

Membrane potential of the SMC (mV):

$$\frac{dv_i}{dt} = -\gamma_v(J_{NaK_i} + J_{Cl_i} + 2J_{VOCC_i} + J_{Na/Ca_i} + J_{K_i} + J_{stretch_i} + J_{KIR_i}) + V_{coupling_i}^{SMC-EC} \quad (120)$$

Open state probability of  $\text{Ca}^{2+}$ -activated  $K^+$  channels (-):

$$\frac{dw_i}{dt} = \lambda_i(K_{act_i} - w_i) \quad (121)$$

$\text{IP}_3$  concentration in the SMC ( $\mu\text{M}$ ):

$$\frac{dIP_{3i}}{dt} = -J_{degrad_i} + J_{IP_3-coupling_i}^{SMC-EC} \quad (122)$$

$K^+$  concentration in the SMC ( $\mu\text{M}$ ):

$$\frac{dK_i}{dt} = J_{NaK_i} - J_{KIR_i} - J_{K_i} \quad (123)$$

The above equation for  $K_i^+$  is redundant since it is not used anywhere else in the SMC. We can use it but it would make any difference.

Arachidonic acid in the SMC, this is just diffused from the astrocyte.

$$\tau_{AA} = \frac{x_{ki}^2}{D_{AA}} \quad (124)$$

$$\frac{dAA_i}{dt} = \frac{AA_k - AA_i}{\tau_{AA}} \quad (125)$$

20-HETE in the SMC

$$\frac{dH_i}{dt} = \frac{1}{1 + \frac{\exp((NO_i - NO_{rest})}{R_{NO}})} \frac{V_a AA_i}{K_a + AA_i} + \frac{V_f AA_i}{K_f + AA_i} - \lambda_h H_i \quad (126)$$

$$(127)$$

Here there are two CYP generators of 20-HETE . The CYP450 generator is inhibited by NO hence the function multiplying the first term of the o.d.e. for 20-HETE. This model is a phenomenological one and relies on the results from [10]

## 7.2 Algebraic Variables

Release of  $\text{Ca}^{2+}$  from  $\text{IP}_3$  sensitive stores in the SMC ( $\mu\text{M s}^{-1}$ ):

$$J_{IP3_i} = F_i \frac{IP3_i^2}{K_{ri}^2 + IP3_i^2} \quad (128)$$

Uptake of  $\text{Ca}^{2+}$  into the SR ( $\mu\text{M s}^{-1}$ ):

$$J_{SR_{uptake_i}} = B_i \frac{Ca_i^2}{c_{bi}^2 + Ca_i^2} \quad (129)$$

$\text{Ca}^{2+}$  induced  $\text{Ca}^{2+}$  release (CICR) ( $\mu\text{M s}^{-1}$ ):

$$J_{CICR_i} = C_i \frac{s_i^2}{s_{ci}^2 + s_i^2} \frac{Ca_i^4}{c_{ci}^4 + Ca_i^4} \quad (130)$$

$\text{Ca}^{2+}$  extrusion by  $\text{Ca}^{2+}$ -ATP-ase pumps ( $\mu\text{M s}^{-1}$ ):

$$J_{extrusion_i} = D_i Ca_i \left( 1 + \frac{v_i - v_d}{R_{di}} \right) \quad (131)$$

Leak current from the SR ( $\mu\text{M s}^{-1}$ ):

$$J_{SR_{leak_i}} = L_i s_i \quad (132)$$

Flux of  $\text{Ca}^{2+}$  exchanging with  $\text{Na}^+$  in the  $\text{Na}^+/\text{Ca}^{2+}$  exchange ( $\mu\text{M s}^{-1}$ ):

$$J_{Na/Ca_i} = G_{Na/Ca_i} \frac{Ca_i}{Ca_i + c_{Na/Cai}} (v_i - v_{Na/Cai}) \quad (133)$$

$\text{Ca}^{2+}$  flux through the stretch-activated channels in the SMC ( $\mu\text{M s}^{-1}$ ):

$$J_{stretch_i} = \frac{G_{stretch}}{1 + \exp \left( -\alpha_{stretch} \left( \frac{\Delta p R}{h} - \sigma_0 \right) \right)} (v_i - E_{SAC}) \quad (134)$$

Flux through the  $\text{Na}^+/\text{K}^+$  pump ( $\mu\text{M s}^{-1}$ ):

$$J_{\text{Na}K_i} = F_{\text{Na}K} \quad (135)$$

$\text{Cl}^-$  flux through the  $\text{Cl}^-$  channel ( $\mu\text{M s}^{-1}$ ):

$$J_{\text{Cl}_i} = G_{\text{Cl}_i} (v_i - v_{\text{Cl}_i}) \quad (136)$$

$\text{K}^+$  flux through  $\text{K}^+$  channel ( $\mu\text{M s}^{-1}$ ):

$$J_{\text{K}_i} = G_{\text{K}_i} w_i (v_i - v_{\text{K}_i}) \quad (137)$$

Flux through inward rectifying  $\text{K}^+$  (KIR) channels in the SMC ( $\mu\text{M s}^{-1}$ ):

$$J_{\text{KIR}_i} = G_{\text{KIR}_i} (v_i - v_{\text{KIR}_i}) \quad (138)$$

$\text{IP}_3$  degradation ( $\mu\text{M s}^{-1}$ ):

$$J_{\text{degrad}_i} = k_{di} \text{IP3}_i \quad (139)$$

Nernst potential of the KIR channel in the SMC (mV):

$$v_{\text{KIR}_i} = z_1 K_p - z_2 \quad (140)$$

Conductance of KIR channel ( $\mu\text{M mV}^{-1} \text{s}^{-1}$ ):

$$G_{\text{KIR}_i} = F_{\text{KIR}_i} \exp(z_5 v_i + z_3 K_p - z_4) \quad (141)$$

Equilibrium distribution of open channel states for the SMC BK channels (-):

$$K_{act_i} = \frac{(Ca_i + c_{w,i})^2}{(Ca_i + c_{w,i})^2 + \alpha_{act_i} \exp(-([v_i - v_{Ca3i} - h_{shift}(H_i - H_0)] / R_{Ki}))} \quad (142)$$

Translation factor, regulatory effect of cyclic guanosine monophosphate (cGMP) on the BK channel open probability ( $\mu\text{M}$ ):

$$c_{w,i} = \frac{\beta_{w,i}}{2} (1 + \tanh \left( \frac{\text{cGMP}_i - \alpha_{w,i}}{\epsilon_{w,i}} \right)) \quad (143)$$

Heterocellular electrical coupling between SMCs and ECs (mV  $\text{s}^{-1}$ ):

$$V_{coupling_i}^{SMC-EC} = -G_{coup}(v_i - v_j) \quad (144)$$

Heterocellular  $\text{IP}_3$  coupling between SMCs and ECs ( $\mu\text{M s}^{-1}$ ):

$$J_{IP_3-coupling_i}^{SMC-EC} = -P_{IP_3} (\text{IP3}_i - \text{IP3}_j) \quad (145)$$

$\text{Ca}^{2+}$  coupling between SMCs and ECs ( $\mu\text{M s}^{-1}$ ):

$$J_{Ca^{2+}-coupling_i}^{SMC-EC} = -P_{Ca^{2+}} (Ca_i - Ca_j) \quad (146)$$

Finally the flux of  $\text{Ca}^{2+}$  through the VOCC channel on the SMC is given by

$$J_{VOCC,i} = g_{VOCC} \frac{v_i - v_{Ca1}}{1 + \exp \left( \frac{-(v_i - v_{Ca2})}{R_{Ca}} \right)} \quad (147)$$

which is the same as equation (111) where  $v_{Ca1} = 100$  mV is the reversal potential,  $v_{Ca2} = -24$  mV is the half-point of the VOCC activation sigmoidal, and  $R_{Ca} = 8.5$  mV is the maximum slope of the sigmoidal (all taken from the NVU model). However for the interneuron model the NPY conductance is given by

$$g_{VOCC} = G_{Ca,i} \left( 1 + \frac{N_{inc}}{2} \tanh \left( \frac{NPY_N - N_{mid}}{N_{slope}} \right) \right) \quad (148)$$

where  $G_{Ca,i} = 1.29 \times 10^{-6} \mu\text{M mV}^{-1} \text{ ms}^{-1}$  is the base conductance of the VOCC (taken from the NVU model),  $N_{inc} = 0.05$  is the proportional increase of the conductance from baseline due to NPY (i.e. 0.05 means a 5% increase from  $G_{Ca,i}$  when NPY is released, model estimate),  $N_{mid} = 0.6$  is the midpoint of the sigmoidal, and  $N_{slope}$  is the slope of the sigmoidal (both model estimates). Hence when  $NPY_N = 0$ ,  $g_{VOCC} = G_{Ca,i}$  and when  $NPY_N = 1$ ,  $g_{VOCC} = 1.05 \times G_{Ca,i}$ .

| Parameter          | Description  | Value   |
|--------------------|--|---|
| $\lambda_i$        | Rate constant for opening  | $45 \text{ s}^{-1}$                                       |
| $F_i$              | Maximal rate of activation-dependent $\text{Ca}^{2+}$ influx                           | $0.23 \mu\text{M s}^{-1}$                                 |
| $K_{ri}$           | Half-saturation constant for agonist-dependent $\text{Ca}^{2+}$ entry                  | $1 \mu\text{M}$   |
| $B_i$              | SR uptake rate constant  | $2.025 \mu\text{M s}^{-1}$                                |
| $c_{bi}$           | Half-point of the SR ATP-ase activation sigmoidal                                      | $1 \mu\text{M}$   |
| $C_i$              | CICR rate constant   | $55 \mu\text{M s}^{-1}$                                   |
| $s_{ci}$           | Half-point of the CICR $\text{Ca}^{2+}$ efflux sigmoidal                               | $2 \mu\text{M}$   |
| $c_{ci}$           | Half-point of the CICR activation sigmoidal  | $0.9 \mu\text{M}$   |
| $D_i$              | Rate constant for $\text{Ca}^{2+}$ extrusion by the ATP-ase pump                       | $0.24 \text{ s}^{-1}$                                     |
| $v_d$              | Intercept of voltage dependence of extrusion ATP-ase                                   | $-100 \text{ mV}$   |
| $R_{di}$           | Slope of voltage dependence of extrusion ATP-ase                                       | $250 \text{ mV}$  |
| $L_i$              | Leak from SR rate constant   | $0.025 \text{ s}^{-1}$                                    |
| $G_{Cai}$          | Whole-cell conductance for VOCCs   | $1.29 \times 10^{-3} \mu\text{M mV}^{-1} \text{ s}^{-1}$  |
| $v_{Ca_{1i}}$      | Reversal potential for VOCCs   | $100 \text{ mV}$  |
| $v_{Ca_{2i}}$      | Half-point of the VOCC activation sigmoidal  | $-24 \text{ mV}$  |
| $R_{Cai}$          | Maximum slope of the VOCC activation sigmoidal   | $8.5 \text{ mV}$  |
| $G_{Na/Cai}$       | Whole-cell conductance for $\text{Na}^+/\text{Ca}^{2+}$ exchange                       | $3.16 \times 10^{-3} \mu\text{M mV}^{-1} \text{ s}^{-1}$  |
| $c_{Na/Cai}$       | Half-point for activation of $\text{Na}^+/\text{Ca}^{2+}$ exchange by $\text{Ca}^{2+}$ | $0.5 \mu\text{M}$   |
| $v_{Na/Cai}$       | Reversal potential for the $\text{Na}^+/\text{Ca}^{2+}$ exchanger                      | $-30 \text{ mV}$  |
| $G_{stretch}$      | Whole cell conductance for stretch activated channels (SACs)                           | $6.1 \times 10^{-3} \mu\text{M mV}^{-1} \text{ s}^{-1}$   |
| $\alpha_{stretch}$ | Slope of stress dependence of the SAC activation sigmoidal                             | $7.4 \times 10^{-3} \text{ mmHg}^{-1}$                    |
| $\Delta p$         | Pressure difference over vessel  | $30 \text{ mmHg}$   |
| $\sigma_0$         | Half-point of the SAC activation sigmoidal   | $500 \text{ mmHg}$  |
| $E_{SAC}$          | Reversal potential for SACs  | $-18 \text{ mV}$  |
| $F_{NaK}$          | Rate of the $\text{K}^+$ influx by the $\text{Na}^+/\text{K}^+$ pump                   | $4.32 \times 10^{-2} \mu\text{M s}^{-1}$                  |
| $G_{Cli}$          | Whole-cell conductance for $\text{Cl}^-$ current                                       | $1.34 \times 10^{-3} \mu\text{M mV}^{-1} \text{ s}^{-1}$  |
| $v_{Cli}$          | Reversal potential for $\text{Cl}^-$ channels  | $-25 \text{ mV}$  |
| $G_{Ki}$           | Whole-cell conductance for $\text{K}^+$ efflux   | $4.46 \times 10^{-3} \mu\text{M mV}^{-1} \text{ s}^{-1}$  |
| $v_{Ki}$           | Nernst potential   | $-94 \text{ mV}$  |
| $k_{di}$           | Rate constant of $\text{IP}_3$ degradation   | $0.1 \text{ s}^{-1}$                                      |
| $F_{KIR_i}$        | Scaling factor of $\text{K}^+$ efflux through the KIR channel                          | $1.285 \times 10^{-6} \mu\text{M mV}^{-1} \text{ s}^{-1}$ |
| $z_1$              | Model estimation for membrane voltage KIR channel                                      | $4.5 \times 10^3 \text{ mV } \mu\text{M}^{-1}$            |
| $z_2$              | Model estimation for membrane voltage KIR channel                                      | $112 \text{ mV}$  |
| $z_3$              | Model estimation for the KIR channel conductance                                       | $4.2 \times 10^{-4} \mu\text{M}^{-1}$                     |
| $z_4$              | Model estimation for the KIR channel conductance                                       | $12.6$  |
| $z_5$              | Model estimation for the KIR channel conductance                                       | $-7.4 \times 10^{-2} \text{ mV}^{-1}$                     |
| $\alpha_{act_i}$   | Translation factor for $v_i$ dependence of $K_{act_i}$ sigmoidal                       | $0.13 \mu\text{M}^2$                                      |
| $v_{Ca_{3i}}$      | Half-point for the $K_{act_i}$ activation sigmoidal                                    | $-27 \text{ mV}$  |
| $R_{Ki}$           | Maximum slope of the $K_{act_i}$ activation sigmoidal                                  | $12 \text{ mV}$   |
| $h_{shift}$        | 20-HETE scaling parameter in $K_{act_i}$ activation sigmoidal                          | $10$  |
| $H_0$              | 20-HETE shift parameter in $K_{act_i}$ activation sigmoidal                            | $0.126 \mu\text{M}$                                       |
| $\lambda_h$        | 20-HETE degradation parameter  | $2.0 \times 10^{-3} \text{ s}^{-1}$                       |
| $\beta_{w,i}$      | Constant to fit data   | $1 \mu\text{M}$   |
| $\alpha_{w,i}$     | Constant to fit data   | $10.75 \mu\text{M}$                                       |
| $\epsilon_{w,i}$   | Constant to fit data   | $0.668 \mu\text{M}$                                       |

|               |   |                       |
|---------------|---|-----------------------|
| $G_{coup}$    | Heterocellular electrical coupling coefficient    | $0.5 \text{ s}^{-1}$  |
| $P_{IP_3}$    | Heterocellular $IP_3$ coupling coefficient        | $0.05 \text{ s}^{-1}$ |
| $P_{Ca^{2+}}$ | Heterocellular $P_{Ca^{2+}}$ coupling coefficient | $0.05 \text{ s}^{-1}$ |

Table 8: Parameters of the SMC compartment, for references see Dormanns et al. [3].

## 8 EC

### 8.1 ODEs

Cytosolic  $Ca^{2+}$  concentration in the EC ( $\mu\text{M}$ ):

$$\begin{aligned} \frac{dCa_j}{dt} = & J_{IP_{3j}} - J_{ER_{uptake_j}} + J_{CICR_j} - J_{extrusion_j} \dots \\ & + J_{ER_{leak_j}} + J_{cation_j} + J_{0j} - J_{stretch_j} - J_{Ca^{2+}-coupling_j}^{SMC-EC} \end{aligned} \quad (149)$$

$Ca^{2+}$  concentration in the ER in the EC ( $\mu\text{M}$ ):

$$\frac{ds_j}{dt} = J_{ER_{uptake_j}} - J_{CICR_j} - J_{ER_{leak_j}} \quad (150)$$

Membrane potential of the EC (mV):

$$\frac{dv_j}{dt} = -\frac{1}{C_{m_j}}(I_{K_j} + I_{R_j}) - V_{coupling_j}^{SMC-EC} \quad (151)$$

$IP_3$  concentration of the EC ( $\mu\text{M}$ ):

$$\frac{dIP_{3j}}{dt} = J_{PLC} - J_{degrad_j} - J_{IP_{3-coupling_j}}^{SMC-EC} \quad (152)$$

### 8.2 Algebraic Variables

Release of  $Ca^{2+}$  from  $IP_3$ -sensitive stores in the EC ( $\mu\text{M s}^{-1}$ ):

$$J_{IP_{3j}} = F_j \frac{IP_{3j}^2}{K_{rj}^2 + IP_{3j}^2} \quad (153)$$

Uptake of  $Ca^{2+}$  into the endoplasmic reticulum ( $\mu\text{M s}^{-1}$ ):

$$J_{ER_{uptake_j}} = B_j \frac{Ca_j^2}{c_{bj}^2 + Ca_j^2} \quad (154)$$

CICR ( $\mu\text{M s}^{-1}$ ):

$$J_{CICR_j} = C_j \frac{s_j^2}{s_{cj}^2 + s_j^2} \frac{Ca_j^4}{c_{cj}^4 + Ca_j^4} \quad (155)$$

$Ca^{2+}$  extrusion by  $Ca^{2+}$ -ATPase pumps ( $\mu\text{M s}^{-1}$ ):

$$J_{extrusion_j} = D_j Ca_j \quad (156)$$

$Ca^{2+}$  flux through the stretch-activated channels in the EC ( $\mu\text{M s}^{-1}$ ):

$$J_{stretch_j} = \frac{G_{stretch}}{1 + \exp\left(-\alpha_{stretch}\left(\frac{\Delta pR}{h} - \sigma_0\right)\right)} (v_j - E_{SAC}) \quad (157)$$

Leak current from the ER ( $\mu\text{M s}^{-1}$ ):

$$J_{ER_{leakj}} = L_j s_j \quad (158)$$

$\text{Ca}^{2+}$  influx through nonselective cation channels ( $\mu\text{M s}^{-1}$ ):

$$J_{cation_j} = G_{cat_j} (E_{Ca_j} - v_j) \frac{1}{2} \left( 1 + \tanh \left( \frac{\log_{10}(Ca_j/c_{log}) - m_{3_{cat_j}}}{m_{4_{cat_j}}} \right) \right) \quad (159)$$

$\text{K}^+$  current through the  $BK_{Caj}$  channel and the  $SK_{Caj}$  channel (fA):

$$I_{K_j} = G_{totj} (v_j - v_{Kj}) (I_{BK_{Caj}} + I_{SK_{Caj}}) \quad (160)$$

$\text{K}^+$  efflux through the  $BK_{Caj}$  channel (-):

$$I_{BK_{Caj}} = 0.2 \left( 1 + \tanh \left( \frac{(\log_{10}(Ca_j/c_{log}) - c)(v_j - b_j) - a_{1j}}{m_{3bj}(v_j + a_{2j}(\log_{10}(Ca_j/c_{log}) - c) - b_j)^2 + m_{4bj}} \right) \right) \quad (161)$$

$\text{K}^+$  efflux through the  $SK_{Caj}$  channel (-):

$$I_{SK_{Caj}} = 0.3 \left( 1 + \tanh \left( \frac{\log_{10}(Ca_j/c_{log}) - m_{3sj}}{m_{4sj}} \right) \right) \quad (162)$$

Residual current regrouping  $\text{Cl}^-$  and  $\text{Na}^+$  current flux (fA):

$$I_{R_j} = G_{R_j} (v_j - v_{restj}) \quad (163)$$

$\text{IP}_3$  degradation ( $\mu\text{M s}^{-1}$ ):

$$J_{degrad_j} = k_{dj} IP3_j \quad (164)$$

### coupling between SMC and EC

membrane coupling

$$V_{coupling_j}^{SMC-EC} = G_{coup} (v_i - v_j) \quad (165)$$

$\text{Ca}^{2+}$  coupling

$$J_{Ca^{2+}-coupling_j}^{SMC-EC} = Ca_{coup} (Ca_i - Ca_j) \quad (166)$$

$\text{IP}_3$  coupling

$$J_{IP_3-coupling_j}^{SMC-EC} = IP_{3,coup} (I_i - I_j) \quad (167)$$

| Parameter | Description   | Value                      |
|-----------|---|----------------------------|
| $J_{0j}$  | Constant $\text{Ca}^{2+}$ influx                                      | $0.029 \mu\text{M s}^{-1}$ |
| $C_{m_j}$ | Membrane capacitance  | $25.8 \text{ pF}$          |
| $J_{PLC}$ | $\text{IP}_3$ production rate   | $0.11 \mu\text{M s}^{-1}$  |
| $F_j$     | Maximal rate of activation-dependent $\text{Ca}^{2+}$ influx          | $0.23 \mu\text{M s}^{-1}$  |
| $K_{rj}$  | Half-saturation constant for agonist-dependent $\text{Ca}^{2+}$ entry | $1 \mu\text{M}$            |
| $B_j$     | ER uptake rate constant   | $0.5 \mu\text{M s}^{-1}$   |
| $c_{bj}$  | Half-point of the SR ATP-ase activation sigmoidal                     | $1 \mu\text{M}$            |
| $C_j$     | CICR rate constant  | $5 \mu\text{M s}^{-1}$     |
| $s_{cj}$  | Half-point of the CICR $\text{Ca}^{2+}$ efflux sigmoidal              | $2 \mu\text{M}$            |
| $c_{cj}$  | Half-point of the CICR activation sigmoidal                           | $0.9 \mu\text{M}$          |
| $D_j$     | Rate constant for $\text{Ca}^{2+}$ extrusion by the ATP-ase pump      | $0.24 \text{ s}^{-1}$      |
| $L_j$     | Rate constant for $\text{Ca}^{2+}$ leak from the ER                   | $0.025 \text{ s}^{-1}$     |

|                |   |  |
|----------------|---|--|
| $G_{catj}$     | Whole-cell cation channel conductivity      | $6.6 \times 10^{-4} \mu\text{M mV}^{-1} \text{s}^{-1}$ |
| $E_{Caj}$      | $\text{Ca}^{2+}$ equilibrium potential      | 50 mV  |
| $c_{log}$      | Log constant                                | $1 \mu\text{M}$  |
| $G_{totj}$     | Total $\text{K}^+$ channel conductivity     | 6927 pS  |
| $v_{Kj}$       | $\text{K}^+$ equilibrium potential          | -80 mV   |
| $m_{3_{catj}}$ | Model constant, further explanation see [9] | -0.18  |
| $m_{4_{catj}}$ | Model constant, further explanation see [9] | 0.37   |
| $c$            | Model constant, further explanation see [9] | -0.4   |
| $b_j$          | Model constant, further explanation see [9] | -80.8 mV   |
| $a_{1j}$       | Model constant, further explanation see [9] | 53.3 mV  |
| $a_{2j}$       | Model constant, further explanation see [9] | 53.3 mV  |
| $m_{3bj}$      | Model constant, further explanation see [9] | $1.32 \times 10^{-3} \text{ mV}^{-1}$                  |
| $m_{4bj}$      | Model constant, further explanation see [9] | 0.30 mV  |
| $m_{3sj}$      | Model constant, further explanation see [9] | -0.28  |
| $m_{4sj}$      | Model constant, further explanation see [9] | 0.389  |
| $G_{Rj}$       | Residual current conductivity               | 955 pS   |
| $v_{restj}$    | Membrane resting potential                  | -31.1 mV   |
| $k_{dj}$       | Rate constant of $\text{IP}_3$ degradation  | $0.1 \text{ s}^{-1}$                                   |
| $G_{coup}$     | coupling coefficient for membrane potential | $0.5 \text{ s}^{-1}$                                   |
| $Ca_{coup}$    | coupling coefficient for $\text{Ca}^{2+}$   | $0.05 \text{ s}^{-1}$                                  |
| $IP_{3,coup}$  | coupling coefficient for $\text{IP}_3$      | $0.05 \text{ s}^{-1}$                                  |

Table 9: Parameters of the EC compartment, for references see Dormanns et al. [3].

## 9 NO pathway

### 9.1 ODEs

$\text{Ca}^{2+}$  concentration in the neuron ( $\mu\text{M}$ ):

$$\frac{dCa_n}{dt} = \frac{1}{1 + \lambda_{\text{buf}}} \left( \frac{I_{\text{Ca,tot}}}{2FV_{\text{spine}}} - \kappa_{\text{ex}}(Ca_n - [Ca]_{\text{rest}}) \right) \quad (168)$$

Activated nNOS ( $\mu\text{M}$ ):

$$\frac{d[\text{nNOS}]_n}{dt} = \frac{V_{\text{max,nNOS}}[\text{CaM}]_n}{K_{\text{m,nNOS}} + [\text{CaM}]_n} - \mu_{\text{deact},n}[\text{nNOS}]_n \quad (169)$$

we have changed some of the parameters for this nNOS equation to get a more reasonable profile see Table 10. These values give a maximum  $n\text{NOS}_{\text{act}}$  of  $0.2408 \mu\text{M}$ . Because of this change initial values for all state variables have been changed (only slightly) to reflect the new values of  $n\text{NOS}_{\text{act}}$  and NO.

NO concentration in the neuron ( $\mu\text{M}$ ):

$$\frac{d\text{NO}_n}{dt} = p_{\text{NO},n} - c_{\text{NO},n} + d_{\text{NO},n} \quad (170)$$

NO concentration in the astrocyte ( $\mu\text{M}$ ):

$$\frac{d\text{NO}_k}{dt} = p_{\text{NO},k} - c_{\text{NO},k} + d_{\text{NO},k} \quad (171)$$

NO concentration in the SMC ( $\mu\text{M}$ ):

$$\frac{d\text{NO}_i}{dt} = p_{NO,i} - c_{NO,i} + d_{NO,i} \quad (172)$$

Activated endothelial NO synthase (eNOS) ( $\mu\text{M}$ ):

$$\frac{d[\text{eNOS}]_j}{dt} = \gamma_{\text{eNOS}} \frac{K_{\text{dis}} C a_j}{K_{m,\text{eNOS}} + C a_j} + (1 - \gamma_{\text{eNOS}}) g_{\max} F_{\text{wss}} - \mu_{\text{deact},j} [\text{eNOS}]_j \quad (173)$$

NO concentration in the EC ( $\mu\text{M}$ ):

$$\frac{d\text{NO}_j}{dt} = p_{NO,j} - c_{NO,j} + d_{NO,j} \quad (174)$$

Fraction of soluble guanylyl cyclase (sGC) in the basal state (-):

$$\frac{dE_b}{dt} = -k_1 E_b \text{NO}_i + k_{-1} E_{6c} + k_4 E_{5c} \quad (175)$$

Fraction of sGC in the intermediate form (-):

$$\frac{dE_{6c}}{dt} = k_1 E_b \text{NO}_i - (k_{-1} + k_2) E_{6c} - k_3 E_{6c} \text{NO}_i \quad (176)$$

Concentration of cGMP in the SMC ( $\mu\text{M}$ ):

$$\frac{dc\text{GMP}_i}{dt} = V_{\max,\text{sGC}} E_{5c} - V_{\max,\text{pde}} \frac{c\text{GMP}_i}{K_{m,\text{pde}} + c\text{GMP}_i} \quad (177)$$

## 9.2 Algebraic Variables

Fraction of open NR2A N-methyl-D-aspartate (NMDA) receptors (-):

$$w_{\text{NR2},A} = \frac{\text{Glu}}{K_{m,A} + \text{Glu}} \quad (178)$$

Fraction of open NR2B NMDA receptors (-):

$$w_{\text{NR2},B} = \frac{\text{Glu}}{K_{m,B} + \text{Glu}} \quad (179)$$

Inward  $\text{Ca}^{2+}$  current per open NMDA receptor (fA):

$$I_{\text{Ca}} = \frac{4v_n G_M (P_{\text{Ca}}/P_M) ([\text{Ca}]_{\text{ex}}/\text{M})}{1 + \exp(\alpha_v(v_n + \beta_v))} \frac{\exp(2v_n/\phi)}{1 - \exp(2v_n/\phi)} \quad (180)$$

Total inward  $\text{Ca}^{2+}$  current for all open NMDA receptors per synapse (fA):

$$I_{\text{Ca,tot}} = (n_{\text{NR2},A} w_{\text{NR2},A} + n_{\text{NR2},B} w_{\text{NR2},B}) I_{\text{Ca}} \quad (181)$$

$\text{Ca}^{2+}$ -calmodulin complex concentration ( $\mu\text{M}$ ):

do we use  $\text{Ca}^{2+}$ -calmodulin complex at all?

$$[\text{CaM}]_n = \frac{C a_n}{m_c} \quad (182)$$

Neuronal NO production flux ( $\mu\text{M s}^{-1}$ ):

$$p_{NO,n} = V_{\max,\text{NO},n} [\text{nNOS}]_n \frac{[O_2]_n}{K_{m,O2,n} + [O_2]_n} \frac{[L\text{Arg}]_n}{K_{m,L\text{Arg},n} + [L\text{Arg}]_n} \quad (183)$$

Neuronal NO consumption flux ( $\mu\text{M s}^{-1}$ ):

$$c_{NO,n} = k_{O2,n}[\text{NO}]_n^2 [O_2]_n \quad (184)$$

Neuronal NO diffusive flux ( $\mu\text{M s}^{-1}$ ):

$$d_{NO,n} = \frac{[\text{NO}]_k - [\text{NO}]_n}{\tau_{nk}} \quad (185)$$

Time for NO to diffuse between the centres of the neuron and the astrocyte (s):

$$\tau_{nk} = \frac{x_{nk}^2}{2D_{c,\text{NO}}} \quad (186)$$

Astrocytic NO production flux ( $\mu\text{M s}^{-1}$ ):

$$p_{NO,k} = 0 \quad (187)$$

Astrocytic NO consumption flux ( $\mu\text{M s}^{-1}$ ):

$$c_{NO,k} = k_{O2,k}[\text{NO}]_k^2 [O_2]_k \quad (188)$$

Astrocytic NO diffusive flux ( $\mu\text{M s}^{-1}$ ):

$$d_{NO,k} = \frac{[\text{NO}]_n - [\text{NO}]_k}{\tau_{nk}} + \frac{[\text{NO}]_i - [\text{NO}]_k}{\tau_{ki}} \quad (189)$$

Time for NO to diffuse between the centres of the astrocyte and the SMC (s):

$$\tau_{ki} = \frac{x_{ki}^2}{2D_{c,\text{NO}}} \quad (190)$$

SMC NO production flux ( $\mu\text{M s}^{-1}$ ):

$$p_{NO,i} = 0 \quad (191)$$

SMC NO consumption flux ( $\mu\text{M s}^{-1}$ ):

$$c_{NO,i} = k_{dno}[\text{NO}]_i \quad (192)$$

SMC NO diffusive flux ( $\mu\text{M s}^{-1}$ ):

$$d_{NO,i} = \frac{[\text{NO}]_k - [\text{NO}]_i}{\tau_{ki}} + \frac{[\text{NO}]_j - [\text{NO}]_i}{\tau_{ij}} \quad (193)$$

sGC kinetics rate constant ( $\text{s}^{-1}$ ):

$$k_4 = C_4[\text{cGMP}]_i^2 \quad (194)$$

Fraction of sGC in the fully activated form (-):

$$E_{5c} = 1 - E_b - E_{6c} \quad (195)$$

Regulatory effect of cGMP on myosin dephosphorylation (-):

$$R_{\text{cGMP}} = \frac{[\text{cGMP}]_i^2}{K_{m,\text{mlcp}}^2 + [\text{cGMP}]_i^2} \quad (196)$$

Maximum cGMP production rate ( $\mu\text{M s}^{-1}$ ):

$$V_{\max,\text{pde}} = k_{\text{pde}}[\text{cGMP}]_i \quad (197)$$

Time for NO to diffuse between the centres of the SMC and the EC (s):

$$\tau_{ij} = \frac{x_{ij}^2}{2D_{c,\text{NO}}} \quad (198)$$

Fraction of the elastic strain energy stored within the membrane (-):

$$F_{\text{wss}} = \frac{1}{1 + \alpha_{\text{wss}} \exp(-W_{\text{wss}})} - \frac{1}{1 + \alpha_{\text{wss}}} \quad (199)$$

Strain energy density (-):

$$W_{\text{wss}} = W_0 \frac{(\tau_{\text{wss}} + \sqrt{16\delta_{\text{wss}}^2 + \tau_{\text{wss}}^2} - 4\delta_{\text{wss}})^2}{\tau_{\text{wss}} + \sqrt{16\delta_{\text{wss}}^2 + \tau_{\text{wss}}^2}} \quad (200)$$

Wall shear stress (Pa):

$$\tau_{\text{wss}} = \frac{R \Delta P}{2L} \quad (201)$$

O<sub>2</sub> concentration in the EC ( $\mu\text{M}$ ):

$$[O_2]_j = c_{\text{unit}} O_2 \quad (202)$$

Oxygen in EC taken as  $O_2$  from lumen (diffusion very fast so plausible!) instead of constant, in  $\mu\text{M}$ , hence  $c_{\text{unit}} = 1$ .

EC NO production flux ( $\mu\text{M s}^{-1}$ ):

$$p_{NO,j} = V_{\text{max,NO},j} [\text{eNOS}]_j \frac{[O_2]_j}{K_{m,O_2,j} + [O_2]_j} \frac{[LArg]_j}{K_{m,L-Arg,j} + [LArg]_j} \quad (203)$$

EC NO consumption flux ( $\mu\text{M s}^{-1}$ ):

$$c_{NO,j} = k_{O_2,j} [\text{NO}]_j^2 [O_2]_j \quad (204)$$

EC NO diffusive flux ( $\mu\text{M s}^{-1}$ ):

$$d_{NO,j} = \frac{[\text{NO}]_i - [\text{NO}]_j}{\tau_{ij}} - \frac{4D_{c,NO} [\text{NO}]_j}{r_l^2} \quad (205)$$

| Parameter                   | Description   | Value  |
|-----------------------------|---|--|
| $[\text{Glu}]_{\text{max}}$ | Maximum glutamate concentration                                       | $1846 \mu\text{M}$                                 |
| $\lambda_{\text{buf}}$      | Buffer capacity   | 20   |
| $V_{\text{spine}}$          | Dendritic spine volume  | $8 \times 10^{-5} \text{ pL}$                      |
| $\kappa_{\text{ex}}$        | Decay rate constant of internal Ca <sup>2+</sup> concentration        | $1.6 \times 10^3 \text{ s}^{-1}$                   |
| $[Ca]_{\text{rest}}$        | Resting internal Ca <sup>2+</sup> concentration                       | $0.1 \mu\text{M}$                                  |
| $V_{\text{max,nNOS}}$       | Maximum nNOS activation rate  | $0.7 \times 10^{-3} \mu\text{M s}^{-1}$ new values |
| $K_{m,\text{nNOS}}$         | Michaelis constant  | $0.8 \mu\text{M}$ new values                       |
| $\mu_{\text{deact},n}$      | Rate constant at which nNOS is deactivated                            | $0.02 \text{ s}^{-1}$ new values                   |
| $K_{m,A}$                   | Michaelis constant  | $650 \mu\text{M}$                                  |
| $K_{m,B}$                   | Michaelis constant  | $2800 \mu\text{M}$                                 |
| $v_n$                       | Neuronal membrane potential   | -40 mV   |
| $G_M$                       | Conductance of NMDA receptor  | $0.46 \text{ pS}$ new value                        |
| $P_{\text{Ca}}/P_M$         | Ratio of Ca <sup>2+</sup> permeability to monovalent ion permeability | 3.6  |
| $[Ca]_{\text{ex}}$          | External Ca <sup>2+</sup> concentration                               | $2 \times 10^3 \mu\text{M}$                        |
| $[\text{M}]$                | Concentration of monovalent ions                                      | $1.3 \times 10^5 \mu\text{M}$                      |
| $\alpha_v$                  | Voltage-dependent Mg <sup>2+</sup> block parameter                    | $-0.08 \text{ mV}^{-1}$                            |
| $\beta_v$                   | Voltage-dependent Mg <sup>2+</sup> block parameter                    | 20 mV  |
| $n_{\text{NR2},A}$          | Average number of NR2A NMDA receptors                                 | 0.63   |
| $n_{\text{NR2},B}$          | Average number of NR2B NMDA receptors                                 | 11   |
| $m_c$                       | Number of Ca <sup>2+</sup> ions bound per calmodulin                  | 4  |
| $V_{\text{max,NO},n}$       | Maximum catalytic rate of neuronal NO production                      | $4.22 \text{ s}^{-1}$                              |
| $[O_2]_n$                   | O <sub>2</sub> concentration in the neuron                            | $200 \mu\text{M}$                                  |

|                 |   |   |
|-----------------|---|---|
| $K_{m,O_2,n}$   | Michaelis constant for nNOS for O <sub>2</sub>                                  | 243 $\mu\text{M}$                                   |
| $[LArg]_n$      | L-Arg concentration in the neuron   | 100 $\mu\text{M}$                                   |
| $K_{m,LArg,n}$  | Michaelis constant for nNOS for LArg  | 1.5 $\mu\text{M}$                                   |
| $k_{O_2,n}$     | O <sub>2</sub> reaction rate constant   | $9.6 \times 10^{-6} \mu\text{M}^{-2} \text{s}^{-1}$ |
| $x_{nk}$        | Distance between centres of neuron and astrocyte                                | 25 $\mu\text{m}$                                    |
| $k_{O_2,k}$     | O <sub>2</sub> reaction rate constant   | $9.6 \times 10^{-6} \mu\text{M}^{-2} \text{s}^{-1}$ |
| $[O_2]_k$       | O <sub>2</sub> concentration in the astrocyte                                   | 200 $\mu\text{M}$                                   |
| $x_{ki}$        | Distance between centres of astrocyte and SMC compartments                      | 25 $\mu\text{m}$                                    |
| $k_{-1}$        | sGC kinetics rate constant  | 100 $\text{s}^{-1}$                                 |
| $k_1$           | sGC kinetics rate constant  | $2 \times 10^3 \mu\text{M}^{-1} \text{s}^{-1}$      |
| $k_2$           | sGC kinetics rate constant  | 0.1 $\text{s}^{-1}$                                 |
| $k_3$           | sGC kinetics rate constant  | $3 \mu\text{M}^{-1} \text{s}^{-1}$                  |
| $V_{\max,sGC}$  | Maximal cGMP production rate  | 0.8520 $\mu\text{M s}^{-1}$                         |
| $K_{m,pde}$     | Michaelis constant  | 2 $\mu\text{M}$                                     |
| $k_{dno}$       | Constant reflecting the activity of various NO scavengers                       | 0.01 $\text{s}^{-1}$                                |
| $C_4$           | sGC rate scaling constant   | $0.011 \mu\text{M}^{-2} \text{s}^{-1}$              |
| $K_{m,mlcp}$    | Hill coefficient  | 5.5 $\mu\text{M}$                                   |
| $k_{pde}$       | Phosphodiesterase rate constant   | 0.0195 $\text{s}^{-1}$                              |
| $x_{ij}$        | Distance between centres of SMC and EC compartments                             | 3.75 $\mu\text{m}$                                  |
| $\gamma_{eNOS}$ | Relative strength of the Ca <sup>2+</sup> dependent pathway for eNOS activation | 0.1   |
| $\mu_{deact,j}$ | eNOS-caveolin association rate  | 0.0167 $\text{s}^{-1}$                              |
| $K_{dis}$       | eNOS-caveolin disassociation rate   | $0.09 \mu\text{M s}^{-1}$                           |
| $K_{m,eNOS}$    | Michaelis constant  | 0.45 $\mu\text{M}$                                  |
| $g_{\max}$      | Maximum wall-shear-stress-induced eNOS activation                               | 0.06 $\mu\text{M s}^{-1}$                           |
| $\alpha_{wss}$  | Zero shear open channel constant  | 2   |
| $W_0$           | Shear gating constant   | 1.4 Pa <sup>-1</sup>                                |
| $\delta_{wss}$  | Membrane shear modulus  | 2.86 Pa   |
| $V_{\max,NO,j}$ | Maximum catalytic rate of NO production   | 1.22 $\text{s}^{-1}$                                |
| $K_{m,O_2,j}$   | Michaelis constant for eNOS for O <sub>2</sub>                                  | 7.7 $\mu\text{M}$                                   |
| $[LArg]_j$      | L-Arg concentration in the neuron   | 100 $\mu\text{M}$                                   |
| $K_{m,L-Arg,j}$ | Michaelis constant for L-Arg  | 1.5 $\mu\text{M}$                                   |
| $\Delta P/L$    | Pressure drop over length of arteriole  | $9.1 \times 10^{-2} \text{ Pa } \mu\text{m}^{-1}$   |
| $k_{O_2,j}$     | O <sub>2</sub> reaction rate constant   | $9.6 \times 10^{-6} \mu\text{M}^{-2} \text{s}^{-1}$ |
| $D_{c,NO}$      | NO diffusion coefficient  | 3300 $\mu\text{m}^2 \text{s}^{-1}$                  |
| $r_l$           | Constant of lumen radius  | 25 $\mu\text{m}$                                    |

Table 10: Parameters of the NO submodel, for references see Dormanns et al. [2].

## 10 AA 20-HETE NO pathway

In our previous model we noted that the rate of increase of  $nNOS_{act}$  and NO was linear and reached a peak at 3 seconds after stimulation. we found a mistake in the NMDA receptor conductance value  $g_{Ca}$  (in the code) . This allowed for  $C_{neuron}$  to be about  $6\mu\text{M}$  which is similar to that found by [18] for 10 receptors per post-synapse. The new values ( in red in Table 10) provide a maximum of  $nNOS_{act} = 0.25\mu\text{M}$  and a maximum of  $NO = 0.13\mu\text{M}$ .

Our results have so far indicated that the NO-cGMP pathway is very slow (even when using experimental data from [22]). This has led to a reconsideration of the NO model and an investigation into the relationship between NO, as a

vasodilator and 20-HETE as a vasoconstrictor. Liu et al [10] provides an hypothesis on the relationship between NO and 20-HETE and EETs in neurovascular coupling. This is illustrated in Figure 20. The key for vasoconstriction is the modulation (inhibition) of the  $K_{Ca}$  channel by 20-HETE. Whilst in contrast NO in addition to the cGMP pathway inhibits the production of 20-HETE from arachidonic acid (AA) via the CYP4A enzyme. In this hypothesis AA diffuses to the SMC from the astrocyte. Using the model of Haffield et al [5] we can write conservation equations for AA and 20-HETE as shown below.

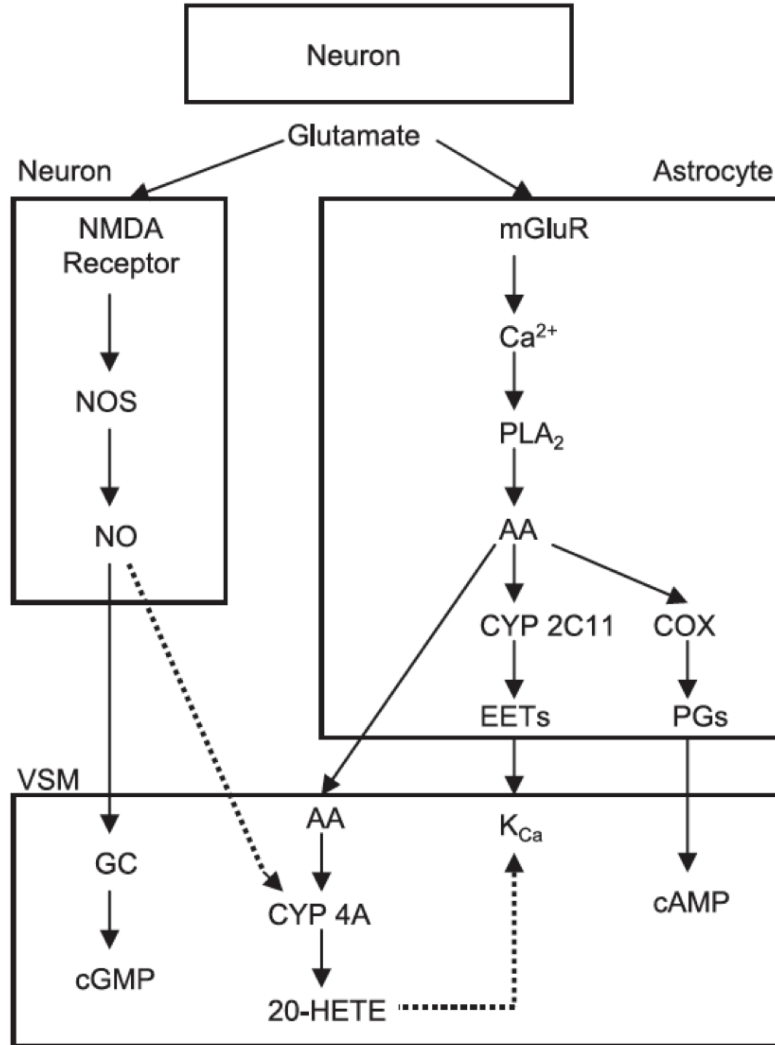


Figure 20: proposed pathway sketch by Liu et al [10] of 20-HETE and NO. Dashed lines are inhibition

$$[AA] = [AA]_b + \frac{AA_{max} \Delta [Ca^{2+}]}{AA_M} \quad (206)$$

$$\frac{d}{dt}[20 - HETE] = f_{NO} \frac{V_{A11}[AA]}{K_{A11} + [AA]} + \frac{V_{F2}[AA]}{K_{F2} + [AA]} - \mu[20 - HETE] \quad (207)$$

$$f_{NO} = \frac{1}{1 + \exp\left(\frac{NO_i - NO_{rest}}{R_{NO}}\right)} \quad (208)$$

The first RHS two terms are based on the fact that both CYPA2 and CYPF2 enzymes contribute to the 20-HETE production. Nitric Oxide degrades the CYPA2 enzyme and hence the function  $f_{NO}$  provides a phenomenological way of

expressing this degradation. The parameter values are given in the Table below

| Parameter   | Description                              | Value                |
|-------------|--|----------------------|
| $[AA]_b$    | archidonic acid baseline                 | $9.3 \mu M$          |
| $AA_M$      | Michaelis constant                       | $0.161 \mu M$        |
| $AA_{max}$  | AA max reaction rate                     | $29 \mu M$           |
| $V_{A11}$   | CYPA 20-HETE max reaction rate           | $0.212 s^{-1}$       |
| $K_{A11}$   | CYPA Michaelis constant                  | $228 \mu M$          |
| $V_{F2}$    | CYPF 20-HETE max reaction rate           | $0.0319 s^{-1}$      |
| $K_{F2}$    | CYPF Michaelis constant                  | $23.5 \mu M$         |
| $\lambda$   | 20-HETE decay constant                   | $0.139 s^{-1}$       |
| $D_{AA}$    | Diffusion coefficient of AA <sup>1</sup> | $10^{-8} m^2 s^{-1}$ |
| $NO_{rest}$ | NO resting concentration for $f_{NO}$    | $0.02047 \mu M$      |
| $R_{NO}$    | saling parameter for $f_{NO}$            | $0.02 s^{-1}$        |

Table 11: parameter values for the production of archidonic acid and 20-HETE.

## 11 Wall mechanics

### 11.1 ODEs

Fraction of free phosphorylated cross-bridges (-):

$$\frac{d[MP]}{dt} = \chi_w (K_4[AMP] + K_1[M] - (K_2 + K_3)[MP]) \quad (209)$$

Fraction of attached phosphorylated cross-bridges (-):

$$\frac{d[AMP]}{dt} = \chi_w (K_3[MP] + K_6[AM] - (K_4 + K_5)[AMP]) \quad (210)$$

Fraction of attached dephosphorylated cross-bridges (-):

$$\frac{d[AM]}{dt} = \chi_w (K_5[AMP] - (K_7 + K_6)[AM]) \quad (211)$$

Vessel radius ( $\mu M$ ):

$$\frac{dR}{dt} = \frac{R_{init}}{\eta} \left( \frac{RP_T}{h} - E \frac{R - R_0}{R_0} \right) \quad (212)$$

### 11.2 Algebraic Variables

Fraction of free non-phosphorylated cross-bridges (-):

$$[M] = 1 - [AM] - [AMP] - [MP] \quad (213)$$

Rate constants for phosphorylation of M to Mp and of AM to AMP ( $s^{-1}$ ):

$$K_1 = K_6 = \gamma_{cross} C a_i^{n_{cross}} \quad (214)$$

<sup>1</sup>Kong et al Fluid Phase Equilibria, 297(3)pp 162-167

Rate constants for dephosphorylation of Mp to M and of AMp to AM ( $\text{s}^{-1}$ ):

$$K_2 = K_5 = \delta_K (k_{\text{mlpc,b}} + k_{\text{mlpc,c}} R_{\text{cGMP}}) \quad (215)$$

Wall thickness of the vessel ( $\mu\text{m}$ ):

$$h = 0.1R \quad (216)$$

Fraction of attached myosin cross-bridges (-):

$$F_r = [AM_p] + [AM] \quad (217)$$

Young's modulus (Pa):

$$E = E_{\text{pas}} + F_r (E_{\text{act}} - E_{\text{pas}}) \quad (218)$$

Initial radius ( $\mu\text{m}$ ):

$$R_0 = R_{\text{init}} + F_r (\alpha_R - 1) R_{\text{init}} \quad (219)$$

| Parameter               | Description  | Value                                |
|-------------------------|--|--------------------------------------|
| $\chi_w$                | Scaling constant for wall mechanics                                | 1.7                                  |
| $K_3$                   | Rate constant for attachment of phosphorylated crossbridges        | $0.4 \text{ s}^{-1}$                 |
| $K_4$                   | Rate constant for detachment of phosphorylated crossbridges        | $0.1 \text{ s}^{-1}$                 |
| $K_7$                   | Rate constant for detachment of dephosphorylated crossbridges      | $0.1 \text{ s}^{-1}$                 |
| $\gamma_{\text{cross}}$ | Sensitivity of the contractile apparatus to $\text{Ca}^{2+}$       | $17 \mu\text{M}^{-3}\text{s}^{-1}$   |
| $n_{\text{cross}}$      | Fraction constant of the phosphorylation crossbridge               | 3                                    |
| $\delta_K$              | Constant to fit data   | 58.14                                |
| $k_{\text{mlpc,b}}$     | Basal MLC dephosphorylation rate constant                          | $8.6 \times 10^{-3} \text{ s}^{-1}$  |
| $k_{\text{mlpc,c}}$     | First-order rate constant for cGMP regulated MLC dephosphorylation | $32.7 \times 10^{-3} \text{ s}^{-1}$ |
| $\eta$                  | Viscosity  | $10^4 \text{ Pa s}$                  |
| $P_T$                   | Transmural pressure  | $4 \times 10^3 \text{ Pa}$           |
| $E_{\text{pas}}$        | Young's moduli for the passive vessel                              | $66 \times 10^3 \text{ Pa}$          |
| $E_{\text{act}}$        | Young's moduli for the active vessel                               | $233 \times 10^3 \text{ Pa}$         |
| $\alpha_R$              | Scaling factor for initial radius                                  | 0.6                                  |

Table 12: Parameters of the wall mechanics submodel, for references see Dormanns et al. [3].

## 12 Tissue Slice Model

### 12.1 ODEs

$\text{K}^+$  concentration in the astrocyte of NVU block  $i$  with four neighbours  $j$  ( $\mu\text{M}$ ):

$$\frac{dK_k^i}{dt} = -\frac{1}{\Delta x} \sum_j J_{K,i \rightarrow j} - J_{K_k}^i + 2J_{NaK_k}^i + J_{NKCC1_k}^i + J_{KCC1_k}^i \quad (220)$$

Membrane potential in the astrocyte of NVU block  $i$  with four neighbours  $j$  (mV):

$$\frac{dv_k^i}{dt} = \gamma_v \left[ -\frac{1}{\Delta x} \sum_j z_K J_{K,i \rightarrow j} - J_{BK_k}^i - J_{K_k}^i - J_{Cl_k}^i - J_{NBC_k}^i - J_{Na_k}^i - J_{NaK_k}^i - 2J_{TRPV_k}^i \right] \quad (221)$$

$K^+$  concentration in the ECS of NVU block  $i$  with four neighbours  $j$  (mM):

$$\frac{dK_e^i}{dt} = -\frac{1}{\Delta x} \sum_j J_{K,i \rightarrow j}^e + \frac{1}{Ff_e} \left( \frac{A_s I_{K,tot_{sa}}^i}{V_s} + \frac{A_d I_{K,tot_d}^i}{V_d} \right) - \frac{dBuff_e^i}{dt} \quad (222)$$

$Na^+$  concentration in the ECS of NVU block  $i$  with four neighbours  $j$  (mM):

$$\frac{dNa_e^i}{dt} = -\frac{1}{\Delta x} \sum_j J_{Na,i \rightarrow j}^e + \frac{1}{Ff_e} \left( \frac{A_s I_{Na,tot_{sa}}^i}{V_s} + \frac{A_d I_{Na,tot_d}^i}{V_d} \right) \quad (223)$$

## 12.2 Algebraic Variables

Gap junction flux of  $K_k$  from NVU block  $i$  to neighbour  $j$  ( $\mu Mm s^{-1}$ ):

$$J_{K,i \rightarrow j} = -\frac{D_{gap}}{\Delta x^2} \left( (K_k^j - K_k^i) + \frac{z_K F}{RT} \frac{K_k^i + K_k^j}{2} (v_k^j - v_k^i) \right) \quad (224)$$

Extracellular electrodifusive flux of  $K_e$  and  $Na_e$  from NVU block  $i$  to neighbour  $j$  ( $Mm s^{-1}$ ):

$$J_{K,e,i \rightarrow j}^e = -\frac{D_{K,e}}{\Delta x} \left[ (K_e^j - K_e^i) - z_K \left( \frac{K_e^i + K_e^j}{2} \right) \left( \frac{z_K D_{K,e} (K_e^j - K_e^i) + z_{Na} D_{Na,e} (Na_e^j - Na_e^i)}{z_K^2 D_{K,e} \frac{K_e^i + K_e^j}{2} + z_{Na}^2 D_{Na,e} \frac{Na_e^i + Na_e^j}{2}} \right) \right] \quad (225)$$

$$J_{Na,e,i \rightarrow j}^e = -\frac{D_{Na,e}}{\Delta x} \left[ (Na_e^j - Na_e^i) - z_{Na} \left( \frac{Na_e^i + Na_e^j}{2} \right) \left( \frac{z_K D_{K,e} (K_e^j - K_e^i) + z_{Na} D_{Na,e} (Na_e^j - Na_e^i)}{z_K^2 D_{K,e} \frac{K_e^i + K_e^j}{2} + z_{Na}^2 D_{Na,e} \frac{Na_e^i + Na_e^j}{2}} \right) \right] \quad (226)$$

| Parameter    | Description                                   | Value                           |
|--------------|---|---------------------------------|
| $D_{gap}$    | Astrocytic gap junction diffusion coefficient | $3.1 \times 10^{-9} m^2 s^{-1}$ |
| $\Delta x^2$ | Width of one NVU block                        | $1.24 \times 10^{-4} m$         |
| $D_{K,e}$    | Extracellular $K^+$ diffusion coefficient     | $3.8 \times 10^{-9} m^2 s^{-1}$ |
| $D_{Na,e}$   | Extracellular $Na^+$ diffusion coefficient    | $2.5 \times 10^{-9} m^2 s^{-1}$ |

Table 13: Parameters of the large scale tissue slice model.

## 13 Initial values

These initial values take into account the new  $nNOS_{act_j}$  and  $NO$  equations. All concentrations are in micromolar and membrane potential in millivolts.

### 13.1 Neuron

$E_t = 0$ ;  $I_t = 0$ ;  $K_e = 3.5$ ;  $Na_{sa} = 9.37$ ;  $Na_d = 9.42$ ;  $O2 = 0.02566$ ;  $CBV = 1.204$ ;  $HbR = 0.7641$ ;  $Ca_n = 0.1$ ;  $nNOS_{act_n} = 0.01056$ ;  $NO_n = 0.02425$ ;

## 13.2 Astrocyte

$Na_k = 18740; K_k = 92660; HCO_{3k} = 9085; Cl_k = 8212; Na_s = 149200; K_s = 2932; HCO_{3s} = 16980; K_p = 3039;$   
 $w_k = 8.26e-5; Ca_k = 0.1435; s_k = 480.8; h_k = 0.4107; I_k = 0.048299; eet_k = 0.4350; m_k = 0.513; Ca_p = 1853; NO_k = 0.02234; v_k = -88.79;$

## 13.3 SMC/EC

$Ca_i = 0.2641; s_i = 1.1686; v_i = -34.7; w_i = 0.2206; I_i = 0.275; K_i = 99994.8; NO_i = 0.02047; E_b = 0.6372; E_{6c} = 0.2606; cGMP_i = 6.1; Ca_j = 0.8339; s_j = 0.6262; v_j = -68.39; I_j = 0.825; eNOS_{act_j} = 0.4451; NO_j = 0.02051;$

## References

- [1] Anenberg, E., Chan, A. W., Xie, Y., LeDue, J. M., and Murphy, T. H. (2015). Optogenetic stimulation of GABA neurons can decrease local neuronal activity while increasing cortical blood flow. *Journal of Cerebral Blood Flow and Metabolism*, 35(10):1579–1586.
- [2] Dormanns, K., Brown, R. G., and David, T. (2016). The role of nitric oxide in neurovascular coupling. *Journal of theoretical biology*, 394:1–17.
- [3] Dormanns, K., van Disseldorp, E. M. J., Brown, R. G., and David, T. (2015). Neurovascular coupling and the influence of luminal agonists via the endothelium. *Journal of Theoretical Biology*, 364:49–70.
- [4] Farr, H. and David, T. (2011). Models of neurovascular coupling via potassium and EET signalling. *Journal of theoretical biology*, 286(1):13–23.
- [5] Hadfield, J., Plank, M. J., and David, T. (2013). Modeling Secondary Messenger Pathways in Neurovascular Coupling. *Bulletin of Mathematical Biology*, 75(3):428–443.
- [6] Hertz, L. (2013). The glutamate-glutamine (GABA) cycle: Importance of late postnatal development and potential reciprocal interactions between biosynthesis and degradation. *Frontiers in Endocrinology*, 4(MAY):1–16.
- [7] Kelsom, C. and Lu, W. (2013). Development and specification of GABAergic cortical interneurons. *Cell and Bioscience*, 3(1):1.
- [8] Kenny, A., Plank, M. J., and David, T. (2018). The role of astrocytic calcium and TRPV4 channels in neurovascular coupling. *Journal of Computational Neuroscience*, 44(1):97–114.
- [9] Koenigsberger, M., Sauser, R., Bény, J.-L. J. L., and Meister, J.-J. J. J.-J. (2006). Effects of arterial wall stress on vasomotion. *Biophysical journal*, 91(September):1663–1674.
- [10] Liu, X., Li, C., Falck, J. R., Roman, R. J., Harder, D. R., and Koehler, R. C. (2008). Interaction of nitric oxide, 20-HETE, and EETs during functional hyperemia in whisker barrel cortex. *American journal of physiology. Heart and circulatory physiology*, 295(2):H619—31.
- [11] Losi, G., Mariotti, L., and Carmignoto, G. (2014). GABAergic interneuron to astrocyte signalling: A neglected form of cell communication in the brain. *Philosophical Transactions of the Royal Society B: Biological Sciences*, 369(1654).

- [12] Mathias, E., Kenny, A., Plank, M. J., and David, T. (2018). Integrated models of neurovascular coupling and BOLD signals: Responses for varying neural activations. *NeuroImage*, 174(March):69–86.
- [13] Mathias, E. J., Plank, M. J., and David, T. (2017). A model of neurovascular coupling and the BOLD response: PART I. *Computer Methods in Biomechanics and Biomedical Engineering*, 20(5):508–518.
- [14] Mizuta, K., Xu, D., Pan, Y., Comas, G., Sonett, J. R., Zhang, Y., Panettieri, R. A., Yang, J., and Emala, C. W. (2008). GABA A receptors are expressed and facilitate relaxation in airway smooth muscle . *American Journal of Physiology-Lung Cellular and Molecular Physiology*, 294(6):L1206–L1216.
- [15] Ostby, I., Oyehaug, L., Einevoll, G. T., Nagelhus, E. A., Plahte, E., Zeuthen, T., Lloyd, C. M., Ottersen, O. P., and Ombolt, S. W. (2009). Astrocytic Mechanisms Explaining Neural-Activity- Induced Shrinkage of Extraneuronal Space. *PLoS Comput. Biol*, 5(1):1–12.
- [16] Petroff, O. A. (2002). GABA and glutamate in the human brain. *Neuroscientist*, 8(6):562–573.
- [17] Samardzic, J., Dragana, J., Hencic, B., Jasna, J., and Svob Strac, D. (2016). GABA/Glutamate Balance: A Key for Normal Brain Functioning. In *InTech*, volume i, page 13.
- [18] Santucci, D. M. and Raghavachari, S. (2008). The effects of NR2 subunit-dependent NMDA receptor kinetics on synaptic transmission and CaMKII activation. *PLoS Computational Biology*, 4(10).
- [19] Schmidt-Wilcke, T., Fuchs, E., Funke, K., Vlachos, A., Muller-Dahlhaus, F., Puts, N. A. J., Harris, R. E., and Edden, R. A. E. (2018). GABA from Inhibition to Cognition: Emerging Concepts. *The Neuroscientist*, 24(5):501–515.
- [20] Uhlirova, H., Kivilvim, K., Tian, P., Thunemann, M., Desjardins, M., Saisan, P. A., Sakadzic, S., Ness, T. V., Mateo, C., Cheng, Q., Weldy, K. L., Razoux, F., Vandenberghe, M., Cremonesi, J. A., Ferri, C. G. L., Nizar, K., Sridhar, V. B., Steed, T. C., Abashin, M., Fainman, Y., Masliah, E., Djurovic, S., Andreassen, O. A., Silva, G. A., Boas, D. A., Kleinfeld, D., Buxton, R. B., Einevol, G. T., Dale, A. M., and Devor, A. (2016). Cell type specificity of neurovascular coupling in cerebral cortex. *eLife (supplementary material)*, 5(MAY2016):1–23.
- [21] Xiong, Z., Bolzon, B. J., and Cheung, D. W. (1993). Neuropeptide Y potentiates calcium-channel currents in single vascular smooth muscle cells. *Pflugers Archiv European Journal of Physiology*, 423:504–510.
- [22] Yang, J., Clark, J. W., Bryan, R. M., and Robertson, C. (2003). The myogenic response in isolated rat cerebrovascular arteries: smooth muscle cell model. *Medical Engineering & Physics*, 25(8):691–709.
- [23] You, J., Edvinsson, L., and Bryan, R. M. (2001). Neuropeptide Y-mediated constriction and dilation in rat middle cerebral arteries. *Journal of Cerebral Blood Flow and Metabolism*, 21(1):77–84.
- [24] Zheng, Y., Pan, Y., Harris, S., Billings, S., Coca, D., Berwick, J., Jones, M., Kennerley, A., Johnston, D., Martin, C., Devonshire, I. M., and Mayhew, J. (2010). A dynamic model of neurovascular coupling: Implications for blood vessel dilation and constriction. *NeuroImage*, 52(3):1135–1147.